



HAL
open science

**A reappraisal of the Poya Terrane (New Caledonia):
Accreted Late Cretaceous-Paleocene marginal basin
upper crust, passive margin sediments and Early Eocene
E-MORB sill complex.**

Dominique Cluzel, Matthew Whitten, Sébastien Meffre, Jonathan C. Aitchison,
Pierre Maurizot

► **To cite this version:**

Dominique Cluzel, Matthew Whitten, Sébastien Meffre, Jonathan C. Aitchison, Pierre Maurizot. A reappraisal of the Poya Terrane (New Caledonia): Accreted Late Cretaceous-Paleocene marginal basin upper crust, passive margin sediments and Early Eocene E-MORB sill complex.. 2017. insu-01565604

HAL Id: insu-01565604

<https://insu.hal.science/insu-01565604>

Preprint submitted on 29 Jul 2017

HAL is a multi-disciplinary open access archive for the deposit and dissemination of scientific research documents, whether they are published or not. The documents may come from teaching and research institutions in France or abroad, or from public or private research centers.

L'archive ouverte pluridisciplinaire **HAL**, est destinée au dépôt et à la diffusion de documents scientifiques de niveau recherche, publiés ou non, émanant des établissements d'enseignement et de recherche français ou étrangers, des laboratoires publics ou privés.

1 ***A reappraisal of the Poya Terrane (New Caledonia): Accreted Late Cretaceous-Paleocene marginal***
2 ***basin upper crust, passive margin sediments and Early Eocene E-MORB sill complex.***

3

4 **Dominique Cluzel¹, Matthew Whitten², Sébastien Meffre³, Jonathan C. Aitchison⁴, Pierre Maurizot⁵**

5

6 ¹University of New Caledonia, BP R4, 98850 Nouméa cedex, New Caledonia,

7 dominique.cluzel@unc.nc

8 ²University of Otago, 362 Leith St, North Dunedin, Dunedin 9016, New Zealand,

9 geologistz55@gmail.com

10 ³University of Tasmania, Sandy Bay campus Private Bag 51, Hobart Tasmania 7001 Australia,

11 smeffre@utas.edu.au

12 ⁴School of Earth and Environmental Sciences, Faculty of Science, The University of Queensland,

13 Brisbane QLD 4072, Australia, jona@uq.edu.au

14 ⁵Geological Survey of New Caledonia, DIMENC B.P. 465, 98845 Nouméa, New Caledonia,

15 pierre.maurizot@gouv.nc

16

17

18 **Abstract**

19 The Poya Terrane of New Caledonia is a composite lithotectonic unit made of i) Campanian-
20 Paleocene E-MORB and BABB-type basalts and abyssal argillite (Poya Terrane Basalts); and ii)
21 Coniacian-Santonian sandstone, turbidites and abyssal argillite (Kone Facies) intruded by Early
22 Eocene E-MORB sills. Remapping reveals that the extent of the Kone Facies is more extensive than
23 previously thought . Field data, petrography and U-Pb geochronology of detrital zircons show that
24 Kone Facies sediments have the same provenance as coeval autochthonous sediments (Formation a
25 Charbon), albeit with more abundant contemporaneous zircons. They accumulated on the eastern
26 continental slope of the Norfolk Ridge, and eventually mixed with abyssal argillite. Temporally, sill
27 emplacement is related to subduction inception at ca. 56 Ma, thus suggesting a possible genetic link.
28 We postulate that either: i) E-MORB intrusion was related to oblique extension and thinning of the
29 down going plate; or alternatively, ii) the “enriched” (off axis?) partial melt zone of the ancient ridge
30 swept the lower plate continentward, generating E-MORB dikes in the upper marginal basin crust,
31 and sills in passive margin sediments before it became extinct. Thereafter, sliced marginal basin
32 upper crust, passive margin sediments and associated dolerite sills were obliquely accreted to the
33 fore-arc region, and in the NE part of the terrane, subducted and recrystallized into the blueschist
34 facies. The Poya Terrane was eventually thrust onto the Norfolk Ridge when the latter reached the
35 subduction zone and debris from the thrust sheet fed mid- to Late Eocene syntectonic basins. At the
36 same time, mafic portions of the Poya Terrane were subducted at depth where they recrystallized

37 into the eclogite facies, mixed with serpentinite to form the Pouebo mélange, and finally were
38 exhumed in the fore-arc region. Finally, Late Oligocene faulting and hydrothermal events overprinted
39 the NE part of the terrane in probable connection with post-obduction granitoid emplacement.

40

41 **Keywords**

42 New Caledonia, obduction, subduction complex, ophiolite, marginal basin, passive margin, accretion,
43 E-MORB sills

44 **Highlights**

45 Poya Terrane of New Caledonia contains slices of Campanian - Late Paleocene marginal basin upper
46 crust (Poya Terrane Basalts) and Coniacian-Santonian passive margin sediments (Kone Facies)

47 Poya Terrane originated in the lower plate of the subduction/obduction system and was locally
48 affected by HP-LT metamorphism

49 E-MORB sills were intruded into the ancient passive margin soon after inception of oblique
50 subduction (ca. 56 Ma)

51

52 Introduction

53 In New Caledonia, an extensive mafic allochthon termed Poya Terrane (Cluzel et al, 1994;
54 2001; 2012) underlies the Peridotite Nappe (Avias, 1967), one of the World's largest ultramafic
55 ophiolites. Both structurally overlie autochthonous rocks of the Norfolk Ridge, which originated
56 through Late Cretaceous break off from southeastern Gondwana. In the south of the island,
57 peridotites are locally overlain by ultra-depleted ultramafic and mafic cumulates, which probably
58 formed in a fore-arc setting (Prinzhofer, 1987; Marchesi, et al, 2009; Pirard et al, 2013; Cluzel et al,
59 2016). The Peridotite Nappe is crosscut by Early Eocene supra-subduction dikes (55-50 Ma; Cluzel et
60 al, 2006; 2016). Obduction occurred when the northern tip of the Norfolk Ridge (see below) jammed
61 a NE-dipping subduction zone.

62 In its original definition (Cluzel et al, 1997), the dominantly mafic Poya Terrane, sandwiched
63 between the autochthonous/parautochthonous terranes and the Peridotite Nappe, is composed of
64 tectonically sliced mafic volcanic rocks and abyssal sediments. In contrast with the Peridotite Nappe,
65 the Poya Terrane does not exhibit any supra-subduction zone feature. Conversely, eclogite-facies
66 (e.g. subducted) equivalents of Poya basalts mixed with meta-serpentinite occur in the Eocene HP-LT
67 complex of northern New Caledonia (Pouebo Terrane; Cluzel et al, 2001). Therefore, the Poya
68 Terrane and its high-pressure metamorphic equivalents, represent a subduction complex formed by
69 accretion and subduction of tectonic slices of the lower plate of the Eocene subduction-obduction
70 system (Cluzel et al, 2001).

71 This accretion model is challenged by a recent re-interpretation of the ophiolite complex of
72 New Caledonia, which suggests that both mafic and ultramafic allochthons were tectonically
73 detached from the upper plate. The gravity-driven southwest-directed slide of allochthonous units
74 being triggered by exhumation of HP-LT metamorphic rocks (Lagabrielle et al, 2013). Therefore, a
75 reappraisal of the Poya Terrane has been undertaken, in order to determine its tectonic/geodynamic
76 setting. Special attention has been given to the Koné Facies, a series of fine grained clastic sediments
77 and mafic volcanic rocks, which crops out near Kone and other localities along the west coast, and is
78 closely associated with Poya Terrane basalts. This volcano-sedimentary unit has been largely
79 underestimated in the past and diversely regarded as: i) an autochthonous unit: the Kone Formation
80 of Carroué (1972) and Paris (1981); ii) an integral part of the allochthonous Poya Terrane (the Kone
81 Facies of Maurizot and Vende-Leclerc, 2009); or, iii) a parautochthonous unit: the Kone Terrane
82 (Cluzel et al, 2012b). This study includes remapping of Poya rocks *sensu stricto* and Koné Facies,
83 petrography of sediments, detrital zircon provenance analysis, geochemistry and U-Pb
84 geochronology of mafic shallow intrusive rocks, as well as examination of relationships with HP-LT

85 metamorphic complex, and leading to proposal of a refined tectonic-geodynamic model for the
86 formation of Poya Terrane.

87 **Geological setting**

88 New Caledonia corresponds to the emerged northern part of the Norfolk Ridge, a narrow
89 submarine rise connected southward to New Zealand (Fig 1). This continental fragment rifted from
90 Australia during Late Cretaceous time (Hayes and Ringis, 1973). The main island of New Caledonia is
91 composed of volcanic, sedimentary and metamorphic terranes, which were assembled during two
92 major tectonic events; assembly of an Early Cretaceous tectonic collage, and Paleocene to Late
93 Eocene accretion followed by obduction/collision. Both events included periods of high-pressure
94 metamorphism in connection with plate convergence in subduction zones. In summary, the
95 geological evolution of New Caledonia comprised three main episodes:

96 i) The Gondwanan phase (Permian-Early Cretaceous) is marked by subduction along the SE-
97 Gondwana margin. At that time, proto-New Caledonia was located in a fore-arc region in which
98 volcanic-arc detritus accumulated; while accretion and subduction of oceanic and terrigenous
99 material formed a *mélange* metamorphosed to blueschist facies.

100 ii) During the Late Cretaceous to Eocene, marginal rifting isolated New Caledonia, and several
101 marginal basins opened in possible connection with an eastward-retreating Paleo-Pacific subduction
102 zone. After a period of shallow water terrigenous sedimentation associated with minor rift-related
103 volcanic activity, only pelagic sediments accumulated. A new NE-dipping subduction system initiated
104 to the east of New Caledonia at the Paleocene-Eocene boundary (Cluzel et al, 2006; 2012a). This
105 system generated the eclogite-blueschist complex of northern New Caledonia, consumed the eastern
106 Australian Plate, and eventually ended with Late Eocene obduction, when the northern part of
107 Norfolk Ridge blocked the subduction zone.

108 iii) Finally, during the post-Eocene phase, New Caledonia emerged; this episode mainly
109 corresponds to post-obduction granitoid intrusion, tropical weathering of exhumed rocks, prominent
110 regolith development and minor tectonic events.

111 Pre-Late Cretaceous rocks in New Caledonia occur in three tectonostratigraphic units: Boghen,
112 Koh-Central, and Teremba terranes. The Boghen Terrane is a subduction complex consisting of
113 schistose and disrupted volcanosedimentary rocks, pillow basalt, chert, black shale, sandstone, tuffs,
114 turbiditic greywacke, serpentinite and mafic/ultramafic *mélange*. These rocks have been
115 metamorphosed to a notably higher grade (lower greenschist to blueschist facies) than the adjacent
116 terranes (Cluzel et al., 1994).

117 The Koh-Central Terrane is a disrupted ophiolite suite of Early Permian age (Aitchison et al.,
118 1998) that occurs locally along the central axis of the island. It is composed of gabbro, dolerite, rare
119 plagiogranite, island-arc tholeiites (IAT) and boninite pillow lavas, and undated abyssal chert directly
120 overlying the pillow basalts (the Koh Ophiolite of Meffre et al., 1996). The Koh Ophiolite rocks are
121 overlain by a thick succession of Triassic to Early Cretaceous deep-water volcano-sedimentary rocks
122 including black shale, volcanoclastic turbidite (greywacke), radiolarian-bearing siltstone and chert
123 (Meffre et al., 1996). The terrane has a distal and deep-water character. Middle Triassic (Anisian) and
124 Late Jurassic (Oxfordian-Kimmeridgian) faunas are correlated with those of the New Zealand
125 Murihiku Terrane (Campbell et al., 1985; Meffre, 1995).

126 The Teremba Terrane is a succession of Upper Permian to mid-Jurassic proximal volcanoclastic
127 and volcanic rocks (andesite, dacite and rhyolite). The sedimentary rocks are typically medium-
128 grained volcanoclastic turbidite with only minor argillite, some shallow- water volcanoclastic
129 conglomerate and rare black shale, a few tens of m thick associated with thin quartzose sandstone.
130 The terrane contains abundant faunas closely resembling those of the Murihiku Terrane of New
131 Zealand (Grant-Mackie et al., 1977; Paris 1981, Campbell, 1984; Campbell et al., 1985, 2001; Ballance
132 & Campbell, 1993). The mineral, chemical and isotopic compositions of greywackes suggest that Koh-
133 Central and Teremba sediments are derived from a similar source, identical to volcanic and sub-
134 volcanic rocks of the Teremba Terrane (Adams et al, 2009).

135 The paleogeographic features of the three pre-Late Cretaceous terranes suggest that they
136 formed during an episode of west-dipping subduction. Faunal endemism, shared with New Zealand,
137 and evidence from geochemistry and detrital zircon age data suggest that they are possibly related to
138 an arc/fore-arc system in discontinuous isolation from Australia (Meffre, 1995; Cluzel and Meffre,
139 2002; Adams et al., 2009).

140 A pre-Coniacian unconformity post-dates the final amalgamation of these terranes and
141 exhumation of high-pressure metamorphic rocks of the Boghen Terrane, which occurred between
142 the Albian (~100 Ma) and the Coniacian (~89 Ma) (Adams et al., 2009; Cluzel et al., 2011). Coniacian
143 to Campanian conglomerate, shallow marine coal-bearing sandstones and carbonaceous siltstones,
144 termed "Formation à Charbon", rest with angular unconformity upon eroded older terranes. A
145 temporal correlative of the Formation à Charbon referred to as the Diahot Terrane (Cluzel et al,
146 2001), exists in the HP-LT metamorphic complex of northern New Caledonia (see below).
147 Metasediments of the Diahot Terrane consist of two units, Tondo and Pilou formations. Tondo
148 Formation is chiefly composed of disrupted conglomerate, sandstone and siltstone of possible
149 turbiditic origin. Pilou Formation is much finer-grained and dominantly consists of carbonaceous

150 schists with extremely rare and thin sandstone layers, bimodal volcanic rocks and associated
151 volcanogenic sulfide deposits. Sandstones of the Formation à Charbon and those of Diahot Terrane
152 yield detrital zircon populations derived from: i) Late Cretaceous (Coniacian) sub-contemporaneous
153 volcanic activity; ii) uppermost Lower Cretaceous (Albian) greywackes (?); and, iii) directly underlying
154 basement terranes (Cluzel et al., 2011).

155 The Paleogene evolution of New Caledonia is characterized by progressive inundation due to
156 post-rift thermal subsidence and development of Maastrichtian to mid-Eocene hemi-pelagic to
157 pelagic sedimentation. Meanwhile, marginal basins opened on both sides of the Norfolk Ridge
158 (Tasman Sea, New Caledonia, and South Loyalty-South Fiji basins). Whether ultra-wide extension of
159 the former East Gondwana margin was related to eastward slab retreat is still an unsolved issue (e.g.,
160 Cluzel et al, 2010) because the corresponding Late Cretaceous-Paleocene volcanic-arc remains
161 unknown. Finally, the northern part of New Caledonia entered a new north- or northeast-dipping
162 subduction zone that initiated at ~56 Ma (Cluzel et al, 2012a), and an Eocene high-pressure
163 metamorphic belt developed in the northernmost part of the island. Meanwhile, imbricate thrusting
164 and a foreland bulge provoked southward-propagating basin inversion and prominent erosion in the
165 mid part of the island.

166 The HP-LT belt comprises mafic blueschist and eclogite facies rocks and metasediments that
167 recrystallized in a NE-dipping subduction zone. Maximum Pressures of ca. 24 kbar and temperatures
168 of ca. 650°C are recorded by relict eclogite-facies assemblages (Clarke et al., 1997; Carson et al.,
169 1999; Vitale-Brovarone and Agard, 2013). Peak metamorphic conditions were probably reached
170 during the early Eocene (~44 Ma, U-Pb dating of metamorphic zircon overgrowths; Spandler et al.,
171 2005). Mafic eclogites in the Pouebo mélange have Late Cretaceous to Eocene protolith ages and
172 share geochemical affinities with Poya terrane basalts (Cluzel et al., 2001; Spandler et al., 2005). The
173 high-grade Pouebo eclogites now form the core of a large antiformal structure wrapped by Diahot
174 schists, and are in turn thrust over low grade autochthonous or parautochthonous rocks of the west
175 coast (Fig 2A). Exhumation of HP-LT metamorphic rocks likely occurred along the subduction channel
176 (Cluzel et al, 2012; Vitale-Brovarone and Agard, 2013) and took place between 40 Ma and about 34
177 Ma, as indicated by U-Pb on zircon, $^{40}\text{Ar}/^{39}\text{Ar}$ on phengite and apatite fission tracks data (Baldwin et
178 al, 2005). The NW-SE trending regional upright foliation, is deformed by km-scale folds with steeply
179 plunging axes (Maurizot et al, 1989; Cluzel et al, 2001), which indicate regional-scale dextral shearing.

180 Meanwhile, two extensive allochthonous terranes, referred to as the Poya Terrane and
181 Peridotite Nappe respectively (Fig. 1 and 2), were successively emplaced during the Eocene. The
182 lower allochthonous unit termed Poya Terrane (or Nappe) (Cluzel et al, 1994, 2001; Aitchison et al,

183 1995a), is a major geological element of New Caledonia, and is exposed on both coasts of the island.
184 The main body is approximately 200 km long and 10 to 25 km wide, and crops out along the west
185 coast. Less extensive units crop out discontinuously along the east coast (Fig. 1). The Poya Terrane
186 comprises massive basalt (flows or sills ?), pillow lavas and abyssal sediment lenses, all of which are
187 locally crosscut by dolerites. The Poya Terrane resulted from off-scraping and slicing of the
188 uppermost levels of the lower plate crust in front of the intra-oceanic Loyalty Arc (Cluzel et al, 2001),
189 forming a mafic subduction complex with some rare interleaved serpentinite lenses (Wakabayashi
190 and Dilek, 2000; Dilek, 2003; Cluzel et al, 2012b). This unit was thrust over autochthonous rocks of
191 the Norfolk Ridge during the Late Eocene as recorded by syntectonic sedimentation in
192 southwestward migrating foreland basins, which contain upwards coarsening units dominated by
193 mafic clasts (Maurizot and Cluzel, 2014). It is worth noting that except in northernmost and slightly
194 older sub basins, which were solely derived from parautochthonous sedimentary units, even the
195 topmost levels (proximal coarse breccia and olistostrome) of the foreland basins always record a
196 mixed sedimentary (parautochthonous sedimentary cover) and magmatic (oceanic crust)
197 provenance. Monogenetic breccias are scarce and only occur in probable connection with collapse of
198 unstable cliffs of basalt, limestone, or black chert. This may denote an origin from a southwestward
199 moving thrust complex composed of both parautochthonous units (Montagnes Blanches Nappe;
200 Maurizot, 2011) and the Poya Terrane. Notably, no component of the Peridotite Nappe exists in
201 syntectonic breccias. The Poya Terrane and autochthonous/parautochthonous terranes were in turn
202 overthrust by the Peridotite Nappe in latest Eocene or earliest Oligocene time (Cluzel et al., 1998).

203 The Peridotite Nappe (Avias, 1967), one of the World's largest ultramafic allochthons,
204 originally covered most of the island. However, several phases of erosion left remnants of tectonic
205 klippen spread along the west coast and a larger unit named "Massif du Sud" in the south of the
206 island. Kinematic indicators in the highly-sheared serpentinite sole, 20-200 m thick, generally indicate
207 top to the SW thrusting (Quesnel et al, 2016). The Peridotite Nappe is dominantly composed of
208 harzburgite (>80%), dunite and minor lherzolite (in northernmost massifs only), which represent
209 elements of a prominently depleted supra-subduction mantle lithosphere (Prinzhofer, 1981).
210 Ultramafic rocks of the Peridotite Nappe display a shallow-dipping compositional layering which
211 locally bears a high-temperature stretching lineation formed by elongated or boudinaged
212 orthopyroxene grains and elongated streaks of chromite with an average N-S trend. Zones of upright
213 high-temperature foliation that locally occur, independently of post-obduction tilt (Bogota Peninsula,
214 Poum and Tiebaghi massifs; Fig 1), have been interpreted as paleo-transform faults (Prinzhofer and
215 Nicolas, 1980; Leblanc, 1995; Titus et al, 2011), which suggest WSW-ESE and WNW-ESE original
216 orientation of the associated spreading ridges.

217 Plagioclase and spinel-bearing lherzolites of the northern massifs, secondarily re-enriched by
218 near-ridge melt circulation, may have generated MORB-like magma (Ulrich et al, 2010; Secchiari et al,
219 2016). In contrast, owing to their extreme depletion in incompatible elements compared to primitive
220 mantle composition, residual harzburgites and dunites, which form the bulk of Peridotite Nappe,
221 underwent over 20-30% partial melting, most probably during several episodes of magma production
222 and cannot have been in equilibrium with MORB-like magma (Prinzhofer and Allègre, 1985; Marchesi
223 et al., 2009; Pirard et al, 2013). Whole rock and mineral chemical constraints allow a complex
224 evolution to be drawn, from re-enrichment by circulating melts during oceanic accretion to mantle
225 metasomatism during subduction (Marchesi et al., 2009; Ulrich et al., 2010; Pirard et al, 2013;
226 Secchiari et al., 2016).

227 Harzburgites and dunites in the Massif du Sud are overlain by dunite, pyroxenite, wehrlite and
228 gabbro cumulates (Prinzhofer, 1987). Cumulate wehrlite and gabbro-norite (enstatite gabbro)
229 probably crystallized from ultra-depleted melts (Marchesi et al., 2009; Pirard et al, 2013). Partial
230 melting and melt fractionation modeling suggest that gabbro-norite cumulates formed in equilibrium
231 with clinoenstatite-bearing boninites. The latter were formed by high-temperature hydrous melting
232 of the mantle wedge enriched by MORB-like slab-derived melts and fluids during the early stage of
233 Eocene subduction (Cluzel et al, 2016). The final melting episode was followed by post-melting
234 diffusion of incompatible elements that may account for extreme depletion of dunites on top of the
235 ultramafic pile (Prinzhofer, 1987; Pirard et al, 2013). It is worth noting that no remnants of earlier
236 MORB-like crust are preserved, and that boninite-related cumulates rest directly upon dunites. The
237 boninitic upper crust itself is not preserved in the present geological record on the island and except
238 for cumulate gabbro, was eroded before/during obduction.

239 Discontinuous amphibolite lenses (100's of m to km in size) pinched between the serpentinite
240 sole and Poya Terrane record recrystallization of oceanic crust rocks (basalt and abyssal argillite) at
241 high temperature (~800-950°C) and low pressure (~0.5 MPa). Amphibolites and crosscutting
242 granulite-facies dikes have a pre-70 Ma protolith and recrystallized at ~56 Ma ($^{40}\text{Ar}/^{39}\text{Ar}$ hornblende
243 and U-Pb zircon and sphene; Cluzel et al., 2012a). Therefore, inception of intra-oceanic subduction
244 that eventually led to obduction occurred in latest Paleocene time within a hot and young oceanic
245 lithosphere; e.g., at or near an oceanic ridge. Amphibolites are geochemically similar to back-arc
246 basin basalts (BABB) characterized by MORB-like REE and trace elements compositions and moderate
247 Nb depletion (Cluzel et al, 2012a) and likely represent the composition of the lower plate crust when
248 it was subducted beneath the hot young lithosphere of the future Loyalty Basin.

249 The Peridotite Nappe is crosscut by a variety of Early Eocene dikes (55-50 Ma; Cluzel et al.,
250 2006), which are not present in the Poya Terrane. These dikes comprise medium to coarse grained
251 rocks, the compositions of which vary from ultramafic (pyroxenite and hornblendite) to felsic (diorite,
252 leucodiorite and granite), and minor basalt (dolerite). The majority of felsic dikes are interpreted to
253 be slab melts formed by partial melting of diverse MORB-like oceanic mafic rocks including gabbro
254 cumulates (Cluzel et al, 2006). However, some of the felsic dikes have geochemical affinity with
255 boninites and have been referred to as “boninite-series”, formed by melting of previously depleted
256 mantle wedge re-enriched by slab melts and fluids (Cluzel et al., 2016). In contrast, the scarce slightly
257 younger (50 Ma) and shallower dolerite dikes, which crosscut gabbro-norite cumulates as well,
258 display supra-subduction affinities (island arc tholeiites, IAT) and likely represent the product of
259 partial melting of “normal” (i.e., fertile) mantle wedge in an infant fore-arc.

260 At variance with widespread opinion (Eissen et al, 1998; Crawford et al, 2003; Lagabrielle et al,
261 2013) boninite is absent from the Poya Terrane and cannot be taken as an evidence for its supra-
262 subduction origin. Actually, the clinoenstatite boninite of Nepoui, which is enclosed in the
263 serpentinite sole, may be genetically related to the Early Eocene supra-subduction dike complex of
264 the Peridotite Nappe, and to gabbro-norite cumulates (Cluzel et al, 2006; 2016). Similarly, the
265 composition of latest Paleocene (56 Ma) high-temperature amphibolites of the metamorphic sole
266 and lower Eocene slab-derived dikes of the Peridotite Nappe suggest that the subducted slab crust
267 had N-MORB or BABB composition.

268 **Loyalty Islands**

269 Considering the geometry and polarity of the Eocene subduction/obduction system, the
270 Loyalty Islands, which represent the emerged part of the largely submarine Loyalty Ridge that runs
271 parallel to the NE of the Norfolk Ridge, for more than 1300 km, likely represent the corresponding
272 volcanic arc (Fig 3). Although this view has been largely accepted, despite many investigations, no
273 rock forming the basement of the Loyalty Islands has been recovered. The only indirect evidence
274 comes from the northern extension of the Loyalty Arc in the South D’Entrecasteaux Zone and in the
275 North Loyalty Basin. In the former, results from ODP sites 830 and 831 indicate that Bougainville
276 Guyot is formed of middle Eocene (40 Ma, $^{40}\text{Ar}/^{39}\text{Ar}$; Mortimer et al. 2014) andesite overlain by 700
277 m thick limestone. DSDP site 286 drilling in the North Loyalty Basin has crosscut 650 m of Middle to
278 Late Eocene volcanoclastic and tuffaceous rocks of volcanic-arc affinity. The continuous morphology
279 of the basin and ridge system and negative gravity anomaly support correlation of the northern and
280 southern parts of this hook-like structure. Based upon this view, a coherent model of evolution of

281 Lord Howe, New Caledonia, and Loyalty ridge and basin system has been suggested (Cluzel et al,
282 2001) and will be taken into consideration in this article (Fig 3).

283 **Post-obduction intrusive rocks**

284 In the south of Grande Terre, two km-size plutons (Saint Louis and Koum) crosscut the
285 Peridotite Nappe and its autochthonous substrate (Fig. 1 and 2) and thus post-date obduction. Saint
286 Louis and Koum plutons display roughly elliptical shapes and are surrounded by a number of m to
287 10's m -thick sub-volcanic dikes. U-Pb zircon geochronology provided Late Oligocene ages for St Louis
288 granodiorite (27.4 ± 0.2 Ma) and Koum granite (24.3 ± 0.1 Ma) as well (U-Pb TIMS; Paquette and Cluzel,
289 2007). Both plutons yielded scarce inherited Paleozoic zircon cores possibly coming from assimilation
290 of basement xenoliths (Paquette and Cluzel, 2007). Late Oligocene granitoids display the geochemical
291 and isotopic features of active margin magmas with almost undecipherable contamination by
292 continental crust rocks shown by Nd-Sr and Pb isotope data. These rocks have been interpreted as a
293 result of short-lived subduction along the west coast accompanied or followed by breakoff of the
294 older slab (Cluzel et al, 2007).

295 Within the Peridotite Nappe, Late Oligocene intrusive rocks are associated with silicification
296 and carbonation of peridotite (listwanite). Both granitoids and listwanite host epithermal and
297 porphyry-type sulphide mineralization. Granitoids and listvenite are the magmatic and hydrothermal
298 consequences of the same event. The occurrence of listwanite associated with epithermal
299 mineralization independently of granitoid outcrops suggests that concealed intrusive bodies may
300 exist at depth. Minor normal faults that crosscut the granitoids, and subsequent transcurrent
301 reactivation highlight post-Oligocene tectonic events also identified along the eastern margin of New
302 Caledonia (Chardon et al, 2008).

303 **Transition between Poya Terrane and Eocene HP-LT metamorphic complex**

304 In northern New Caledonia elements of the Poya Terrane and Peridotite Nappe are involved in
305 recumbent west-verging folds where they form irregular lenses pinched in synclines. The
306 metamorphic grade of these lenses increases from west to east as in the rest of the HP-LT complex.
307 Peridotites form gentle synforms prolonged downward by highly schistose serpentinites pinched in
308 narrow slivers, a few 10s of m thick and several km long (Maurizot & Vende-Leclerc, 2009; Gautier et
309 al, 2016). These peridotite-serpentinite units contain boudinaged and sheared Early Eocene dikes
310 similar to those in the Peridotite Nappe and thus may be directly correlated with it. In contrast, no
311 direct equivalent of the Poya Terrane exists; instead, blocks of dolerite, basalt, red chert and
312 leucodiorite occur within mélangé with a matrix of sheared serpentinite. The eclogitized Pouebo

313 mélange contains m to 100 m size blocks of E-MORB eclogites, which could be metamorphosed
314 dolerites of the Kone Facies (see U-Pb geochronology section below).

315

316 **Transported piggyback basins**

317 Turbidite successions, referred to as the Nepoui-Koumac Flysch and Olistostrome are closely
318 associated with Poya basalts in Nepoui and Koumac areas and likely represent transported piggyback
319 basins (Fig 1; note that these occurrences are too small to be represented on the map). Both basins
320 are tectonically pinched between the Poya Terrane and the Peridotite Nappe. The Nepoui Flysch
321 starts with 2–5 m-thick biocalcarene of imprecise age (Bartonian–Priabonian; Paris et al, 1979;
322 Meffre, 1995; Cluzel et al, 1998) that rests directly upon serpentinite. Significantly, the basal
323 limestone contains large benthic foraminifers, together with some detrital serpentinite and chromite
324 grains. It is overlain by pale brown argillite, and alternating coarse arenite and dolomicrite. On top of
325 arenite beds, thin (2-5 mm) layers or lenses of reworked red argillite, which appear locally, very
326 closely resemble those of the Poya Terrane. Soft sediment deformation (slumps) is widespread.
327 Arenite clasts are derived from three distinct sources: Poya Terrane basalt (clinopyroxene, ilmenite
328 and magnetite), an adjacent shallow water platform (carbonate bioclasts), and serpentinite. It is
329 worth noting that the arenites contain no fresh peridotite rock or ultramafic mineral clasts such as
330 chromite. They also lack any high-pressure metamorphic detritus as well. The fine-grained beds, 2–10
331 cm thick, have yielded an uppermost Eocene (Priabonian) pelagic microfauna). Near Koumac (north)
332 an olistostrome, c. 300 m thick, displays several mass flow units, 5-10 metres thick, composed of
333 basalt boulders embedded in a matrix of sandy breccia made of pillow and chert fragments with
334 some lenses of red blocky argillite. Basalt fragments display the same geochemical features as the
335 dominant facies of Poya basalt (E-MORB; Cluzel et al., 2001). On top of the mass flow unit, a few
336 rafted basalt boulders are overlain by a ~50 m thick section of alternating sands and dolomicrite. The
337 Nepoui-Koumac Flysch probably accumulated in piggyback basins located at, or close to, the
338 boundary between the Poya Terrane and exhumed serpentinites of the fore-arc region. The apparent
339 absence of clasts of terrigenous lithologies of the Koné Facies suggests that flysch formation occurred
340 in connection with Poya basalts before the tectonic amalgamation of Kone and Poya rocks in one
341 single terrane.

342

343 **Poya Terrane and Kone Facies**

344 The large allochthonous unit termed Poya Terrane (Cluzel et al, 1997) crops out along the
345 west coast in a region of low-elevation grasslands, and sporadically, in smaller lenses along the east
346 coast. The Poya Terrane has only scarce and deeply weathered outcrops; however, new man-made
347 exposures due to the economic development of the area reveals that the extent of the dominantly
348 sedimentary component termed Kone Facies had been largely underestimated and actually
349 constitutes about one third of the area/volume of the terrane (Fig 1). The larger units of Kone Facies
350 crop out on the northeastern side of the terrane. However, smaller lenses of clastic sediments also
351 appear at several places tectonically intercalated with basalt and abyssal argillite of undoubtedly
352 oceanic origin. In contrast with the low hills formed by Poya basalts, Kone Facies rocks define steep
353 elongate ridges reinforced by upright dolerite sills, which can be followed over several kms. A
354 detailed field survey confirms that Poya Terrane basalts and Kone Facies rocks are associated in one
355 single tectonic unit thrust upon Late Cretaceous to Eocene autochthonous rocks.

356 The Poya Terrane *sensu stricto* comprises slices of upper oceanic crust (basalt and abyssal
357 sediments), metamorphosed (zeolite to lower greenschist facies) by both burial and “hydrothermal”
358 (ocean floor) metamorphism (Nicholson et al, 2000; Cluzel et al, 2001), and crosscut by a vein
359 network filled with quartz, epidote, chlorite, zeolite and sulfides. Typically red, and more rarely
360 white, green or dark-brown colored cherts and argillites, are dominantly composed of aluminous clay
361 (illite) and zeolite minerals, which may be derived from felsic (suspensions of continental origin or
362 volcanic ashes) and hydrothermally altered mafic (ocean basalt) sources respectively. Small-scale Fe-
363 Mn crusts and polymetallic sulfide ore appear locally. Diversely colored radiolarian cherts appear in
364 coherent beds and in elongated nodules 2-5 cm thick. Abyssal argillites form upright lenses, 20cm to
365 5 m thick, rarely interpillows, never contain macrofossils but yield Campanian to Late Paleocene or
366 earliest Eocene radiolarians (Aitchison et al, 1995b; Cluzel et al, 2001). Clastic rocks directly
367 associated with basalt are rare but significant. Pale red fine-grained quartz-bearing calcarenite 40 cm
368 thick, occurs about halfway between Bourail and Poya, where it is associated with pink limestone and
369 pale red argillite and on the northeastern flank of the Koniambo Massif near Kone (laminated
370 sandstone in red chert). Gray siltstones and argillites 15 m thick also appear at a single locality
371 associated with basalt but are also found associated with coherent Kone Facies unit near Kaala-
372 Gomen. Scarcely, in some sediment lenses, chert beds have been disrupted and form
373 intraformational breccia (mélange) with sub rounded clasts embedded in red abyssal argillite, thus
374 suggesting soft-sediment deformation (online supplementary material, Figure S1d). It is worth noting
375 that such breccias are strictly intraformational and never contains basalt clasts.

376 Some Poya Terrane basalts display the geochemical features of oceanic plateaus (E-MORB) and
377 had been interpreted as such (Cluzel et al, 1997). However, their association with abyssal argillite

378 suggests eruption at depths not less than 3,000 m and they cannot have formed a massive plateau
379 such as Ontong Java (Kroenke, 1972). Instead, eruption of enriched basalts is a feature of some
380 modern SW Pacific back-arc basins, such as Lau Basin (Volpe et al, 1988), and North Fiji Basin (Eissen
381 et al, 1998) and their association with (apparently) minor back-arc basin basalts (Cluzel et al, 2001)
382 supports this interpretation (see discussion below). The dominant proportion (80%) of E-MORBs
383 relative to other basalts types (BABB and OIB) in the database (Cluzel et al, 2001) is probably due to a
384 sampling bias. All these rocks are covered by 5-20 m-thick regolith in which mainly unweathered
385 boulders of dolerite remain; therefore E-MORB dolerites are over-represented compared to other
386 basalt types.

387 According to the original definition, Koné Facies is composed of interbedded, khaki-colored
388 cherts, siltstones and argillites with some fine to medium-grained sandstones (Carroué, 1972; Paris,
389 1981), which actually correspond to distal turbidites. Bed thicknesses are typically 2 to 10 cm, with
390 thickly bedded or massive units rarely encountered (online supplementary material Figure S1, Plate
391 1b). It is worth noting that in contrast to the autochthonous Formation a Charbon of about the same
392 age, Kone Facies has no known basement and faulted boundaries with surrounding rocks are
393 ubiquitous.

394 In contrast with intensely disrupted Poya Terrane sensu stricto, Kone Facies forms large
395 coherent units, and even if continuous sections are rarely over 100 m across and prevent accurate
396 stratigraphic correlations, transition between different lithologies may be observed at several
397 localities. A somewhat abrupt (within 10 m) change from south-dipping sandstone into fine-grained
398 (silt/argillite) turbidite may be observed along the Kone-Tiwaka road (WGS 84: 164.9014; -21.0711;
399 online supplementary material, Fig. S1a). Transition between khaki fine-grained turbidites and red or
400 dark-brown argillite-chert succession similar to the usual Poya abyssal sediments may be observed
401 along the RT1 (main road) to the NW of Bourail (165.428; -21.4906), at Tribu de Boyen (164.615; -
402 20.832) and in many other localities. Therefore, it may be considered that the bulk of Kone Facies
403 rocks represent one single fining-upward sequence evolving from relatively coarse sandstone into
404 distal turbidites and finally abyssal argillite and chert. Sandstones show compositional variation from
405 well-rounded and well-sorted to angular and poorly sorted, with local intra-formational reworking.
406 Lateral continuity is rarely seen over large distances. In contrast with the autochthonous Formation à
407 Charbon, which contains rift-related mafic and felsic volcanic rocks, no contemporaneous volcanic
408 rocks exist in Kone Facies, and carbonaceous rocks are also lacking. The lack of coeval interlayered
409 volcanic rocks (see U-Pb geochronology section below) contrasts with the large zircon population of
410 Late Cretaceous age (see below).

411 The presence of marine macro-fossils, such as inoceramids, and recrystallized radiolarian
412 “ghosts” in chert undoubtedly indicate marine deposition. Although it represents a minor component
413 in the Kone Facies, sandstone is important in respect of the sedimentary processes involved and
414 sediment provenance. Sandstones typically occur in beds, a few mm to a few cm thick (online
415 supplementary material, picture S1, Plate 1a), in which grain size varies from very fine to coarse sand,
416 with the majority of samples comprising grain sizes of 125-500 μm (online supplementary material,
417 picture S1, Plate 2). They are generally well-sorted but display variable grain sphericity and rounding,
418 and generally lack current features such as graded bedding, or cross bedding. The ungraded and
419 laminated nature of the sandstones, overall fine-grain texture, abundance of interbedded cherts and
420 argillites and local synsedimentary deformational structures (slumps, soft sediment boudinage),
421 suggest deposition of sandy turbidites by aggradation from sustained high density mass flows on the
422 continental slope.

423 Quartz and feldspar (albite) are the dominant clastic minerals, cemented by interstitial calcite,
424 which most probably originates from albitisation of detrital feldspar of volcanic origin. Instead, many
425 sandstone samples have been secondarily silicified during burial, diagenesis and dolerite intrusion,
426 and identification of grain boundaries may be difficult. The source of the silica is from both shale and
427 sandstone beds. From shales, the most likely important silica sources include clay transformation,
428 chiefly illitization of smectite, dissolution and pressure solution of detrital grains and dissolution of
429 opaline skeletal grains (radiolarians). From sandstones, silica sources include pressure solution of
430 detrital quartz grains at grain contacts, feldspar alteration and dissolution and possibly carbonate
431 replacement of silicate minerals (McBride, 1989).

432 According to the relative abundances of quartz, feldspar and lithic clasts, sandstones may be
433 loosely categorized in the field as being intermediate between siliciclastic and volcanoclastic. The
434 point counting method on stained polished slabs developed by Gazzi (1966) and Dickinson (1970) has
435 been used together with petrographic analysis of thin sections to characterize more accurately the
436 provenance of sandstones. The Koumac, Koné and Bourail sandstones plot reasonably close to each
437 other within the recycled orogenic section of the diagram and each region is also closely grouped in
438 terms of composition (Fig 4). Sandstones from the Bourail region, for example, are more quartz-rich
439 than sandstones from other localities. The Kaala-Gomen, Temala and Bouloupari sandstones tend to
440 plot on the edges of the Transitional Arc and Dissected Arc fields. However, within each group of
441 outcrops, sandstones of different provenances may appear together. It is worth noting that no rock
442 fragments from the HP-LT Boghen Terrane have been identified, probably because these rocks
443 provide low-resistance clasts, which are commonly not preserved during sedimentary transport. The
444 weak correlation between geographical location and sandstone composition probably results from

445 tectonic disruption and remixing; and the differences that appear between them probably reflect the
446 mixed nature of their source.

447 The composition of argillite beds has been investigated using X-ray powder diffraction (XRD)
448 and short wave infrared (SWIR) spectroscopy. All samples dominantly contain quartz (ca. 30%), and
449 similar contents of albite together with illite, minor smectite and montmorillonite. Illite, which
450 dominates in almost all samples may directly result from the weathering of felsic rocks under cool
451 climate conditions, or indirectly from illitization of smectite during burial diagenesis. As smectite is
452 derived from a mafic igneous source, it is likely that illite in these samples is a product of the
453 illitization process. SWIR analysis also detected the presence of minerals of the mica family; phengite
454 (SiMg-rich aluminous mica), and paragonite (Na-rich aluminous mica) and clinochlore (Mg-rich
455 chlorite). Magnesium-rich phengite is likely to have been produced by illitization of smectite. If so,
456 this same process may have occurred in samples that contain montmorillonite, which is derived from
457 smectite in an alkaline environment. Phengite, paragonite and clinochlore are common mineral of
458 rocks that have been subjected to blueschist facies metamorphism.

459 Available evidence suggests that argillite beds are derived from both mafic and alumina-silicate
460 igneous sources with some contribution of HP-LT metamorphic rocks. Sources potentially exist in the
461 pre-Late Cretaceous terranes of New Caledonia, which contain mixed felsic and mafic volcano-
462 sedimentary rocks (Koh-Central and Teremba terranes) and HP-LT metamorphic rocks (Boghen
463 Terrane) as well.

464 The formation is intruded by dolerite sills, a few meters to 100 m thick, forming elongated
465 ridges, some of which may be traced over several km. The intrusion of dolerite had the effect of
466 locally recrystallizing the sediments (nodular "schist" to hornfels) by contact metamorphism (online
467 supplementary material, Fig. S3a-d). Therefore, finely recrystallized siltstones have sometimes been
468 mistaken for chert. Only one outcrop contained a mafic dike, which crosscuts the bedding. Sills do
469 not display chilled margins and are generally medium grained. Large (50-100 m thick) dolerite sills
470 may be coarse grained in their inner parts with cm-size nodular aggregates of pyroxene and may be
471 termed gabbro (e.g., Audet, 2008; Maurizot and Vende-Leclerc, 2009). Thus, they cooled slowly and
472 were probably not connected upwards to the surface. Dolerite sills locally (i.e., RT1 near Kone, west
473 coast and Thiem Bridge near Touho, east coast) contain large enclaves (up to 10 meters) of fine-
474 grained Kone Facies sediments, totally recrystallized into hornfels. Except in the northern part of east
475 coast units, which have been involved in the Eocene HP-LT complex (see metamorphism section
476 below), dolerite sills never display internal (ductile) deformation or striated boundaries, which could
477 advocate syntectonic emplacement.

478 **Paleontology**

479 Dominantly fine-grained turbidites generally contain few macrofossils. This is also the case for
480 siltstones and argillites of the Koné Facies, which contain scarce external casts of fossil inoceramid
481 shells, some of which reach more than 20 cm in diameter. In spite of their adaptation to a wide range
482 of benthic environments, inoceramids generally tended to live in upper bathyal and neritic
483 ecosystems (Harries et al, 1996). Therefore, their occurrence in deep water distal turbidites is
484 somewhat puzzling unless large thin shells were rafted downslope with the enclosing sediments. The
485 Kone Facies rocks yielded *Inoceramus australis* (Paris, 1981), which represents the Piripauan stage of
486 New Zealand (uppermost Coniacian to Middle Santonian; Crampton et al, 2000), and *Inoceramus*
487 (*Sphaenoceramus*) *angustus* of Upper Santonian-Lower Campanian affinity (Tröger, 2000). These
488 assignments make the Kone Facies almost synchronous with Formation à Charbon (Coniacian-
489 Campanian; Maurizot et al, 2016). In contrast with such relative macrofossil paucity, abundant
490 radiolarians are present in most thin sections of fine-grained siltstone and chert containing circular or
491 elliptical impressions that represent more or less recrystallized radiolarian skeletons. Eighteen
492 representative samples of chert, siltstone and argillite have been digested in diluted HF for extracting
493 radiolarians as a means of constraining the age of the formation. Of the samples etched, radiolarians
494 were recovered from only seven samples. Unfortunately, petrographic and SEM imaging of the
495 extracted radiolarians show that all had been recrystallized and could not be determined. In
496 summary, on the basis of macrofossils only, the Kone Facies may be assigned to the uppermost
497 Coniacian to Lower Campanian (~87-80 Ma), a correlation consistent with detrital zircon data (see
498 below).

499 **Detrital zircon provenance**

500 A detrital zircon study was undertaken on ten representative samples of siliciclastic,
501 volcanoclastic and greywacke-like sandstones. The obtained data were compared to those from the
502 autochthonous Late Cretaceous Formation à Charbon of about the same age. Details of detrital-
503 zircon preparation procedures, LA-ICPMS dating techniques, and U–Pb data treatment are given in
504 Appendix 1.

505 All sandstones contained relatively young, euhedral zircon crystals and older, rounded crystals.
506 The distribution of combined ages of all 225 zircons from the ten samples shows a main Cretaceous
507 population, a lesser Early Mesozoic group and a minor Paleozoic- Precambrian group (Fig 6 and 7
508 and online supplementary material, Fig. S6a & S6b, Table 1). The distribution of Cretaceous zircons
509 shows two distinct age peaks at 104 Ma (Albian) and 83 Ma (Coniacian-Santonian). Age-probability
510 plots for individual samples show that all of the Koné sandstone samples have similar detrital zircon

511 patterns differing mostly in the magnitude of the youngest Coniacian-Santonian population with
512 respect to the Albian and older zircon populations (Fig. 5). The Coniacian-Santonian zircon population
513 is very close to the sediment age determined upon paleontological grounds and likely related to a
514 synchronous magmatic activity, consistent with the volcanoclastic character of most of the
515 sandstones. The prominent Albian zircon population is widespread in Upper Cretaceous sedimentary
516 rocks of New Caledonia (Cluzel et al, 2011) and New Zealand as well (Adams et al, 2013a, 2013b,
517 2016). Albian rocks are only poorly represented in New Caledonia by scarce volcanoclastic turbidites
518 that share the same origin as the rest of Mesozoic greywackes from the basement terranes (Adams
519 et al, 2009; Cluzel et al, 2011). Therefore, Early Cretaceous zircons may locally be derived from
520 volcanic or volcanoclastic rocks that were eroded before the Late Cretaceous; or alternatively, from
521 an external source of this age such as the silicic Eastern Australian Whitsunday Province (Bryan et al,
522 2000; 2012).

523 Zircon age data for the Upper Cretaceous Formation à Charbon similarly displays a predominant
524 Cretaceous and a minor Precambrian-Paleozoic “Gondwanian” population (Adams et al. 2009; Cluzel
525 et al. 2011). In contrast with Kone Facies, the distribution of Cretaceous zircons is not clearly
526 bimodal; however, younger Coniacian and older Albian populations coexist, thus suggesting that the
527 Kone Facies depocenter was closer to the Late Cretaceous volcanic source. The pre-Cretaceous zircon
528 populations slightly differ from place to place depending upon the nature of the directly underlying
529 terrane, thus suggesting local derivation (Cluzel et al, 2011).

530 A formal comparison of pre-Cretaceous zircon age populations of Kone sandstones with
531 individual samples of pre-Late Cretaceous basement terranes using the Kolmogorov-Smirnov test
532 (Whitten, 2015; not presented) shows a greater similarity with zircon populations of greywackes of
533 the basement terranes that crop out on the eastern slopes of New Caledonia (Central Terrane).

534 **Dolerite geochronology**

535 Previous attempts to date Poya Terrane basalts have proven difficult as a consequence of
536 tropical weathering and widespread low grade metamorphism. However, Palaeocene to Eocene K-Ar
537 ages (59 ± 6 to 38.5 ± 1.5 Ma) were suggested by Guillon and Gonord (1972), and more recently
538 (61.6 ± 2.8 to 39.7 ± 2.1 Ma) by Eissen et al (1998). The apparent ages of these slightly metamorphosed
539 rocks are somewhat younger than the fossil (radiolarian) ages obtained from the associated abyssal
540 sediments (83.5-55 Ma; Aitchison et al, 1995; Cluzel et al, 2001); thus, they have been regarded
541 unreliable and discarded. Therefore, without attempting to date the basalts again, in situ LA-ICPMS
542 U-Pb geochronology has been undertaken on micro-zircons of twelve dolerite dikes/sills that crosscut
543 the sediments of Koné Facies and basalts of Poya Terrane (the dating method is summarized in online

544 supplementary material, Text S1). The results show that all the analyzed dolerite dikes/sills
545 crystallized during a relatively narrow time interval in the latest Paleocene and Early Eocene
546 (58.4 ± 1.5 - 47.6 ± 4.0 Ma) (online supplementary material, Data set S2). It is therefore possible that
547 some of the previously obtained K-Ar ages are related to the same magmatic event and come from
548 unmetamorphosed dolerites. With the exception of a few grains (less than 10%), which show some
549 Pb loss, most zircons display concordant U-Pb ages (Fig 7a; 8c). The dolerite U-Pb ages cluster around
550 54 ± 5 Ma (Fig 7b), almost the same age as the younger abyssal sediments of the Poya Terrane, a little
551 bit older than pre-obduction dikes from the Peridotite Nappe (~ 53 Ma, Cluzel et al, 2006) and slightly
552 younger than subduction inception at ~ 56 Ma (Cluzel et al, 2012a).

553 In the Pouebo eclogitized mélange (north), large mafic blocks of dominantly E-MORB affinity
554 are mixed with metaserpentinite (talcschist). Some yielded U-Pb ages on zircon cores of ca. 84 Ma
555 and 55 Ma and recrystallization rims of ca. 44 Ma due to HP-LT metamorphism (Spandler et al, 2005
556 Pirard and Spandler, 2017). Massive eclogite blocks (some may exceed 100 m in size) of the Pouébo
557 mélange, which yield Early Eocene magmatic zircons and E-MORB geochemical features, may have
558 parent rocks in Kone dolerites. In contrast, the detrital zircon component of some metasediments of
559 the Pouebo Terrane indicates probable derivation from Upper Cretaceous sediments (Pirard and
560 Spandler, 2017) but the number of dated zircons (8) is insufficient to be compared to Formation à
561 Charbon or Kone Facies. Therefore, some components of the Pouebo Terrane probably have
562 protoliths coming from the Kone Facies. However, the degree of the metamorphism is of such
563 intensity that metasedimentary rocks derived from the Kone Facies could not be recognized in the
564 field.

565 On the east coast, dolerites crop out discontinuously and are associated with typical fine-
566 grained turbidites of the Kone Facies (online supplementary material, Fig. S5a & S5d), which display
567 contact metamorphism (nodular schist). Some of them display strongly heterogeneous deformation
568 due to transcurrent tectonics and strain partitioning. Undeformed (although metamorphosed) thick
569 dolerites of the Thiem Unit (between Hienghène and Touho; Fig 1) display dominantly concordant
570 zircons with the same age (55.9 ± 1.2 Ma) as the rest of the terrane (Fig 7c). However, severely
571 sheared dolerites of the same group of outcrops yield discordant U-Pb zircon ages that span the 58-
572 19 Ma time interval (sample THIEM 3, online supplementary material, Data set S2). The older
573 population with low U and Th contents is Eocene in age. The younger ones are metamict high U and
574 Th zircons that define a loosely constrained intercept at 26.3 ± 0.6 Ma (Fig 7d). In spite of some
575 uncertainty due to incomplete reset of the zircon U-Pb system, it appears that dolerites of the Thiem
576 Unit were intruded into Kone Facies sediments at ~ 56 Ma, as in the rest of the terrane and have been

577 sheared at ~26 Ma. It is worth noting that the latter event may be time-correlated with Late
578 Oligocene granitoid emplacement (Paquette and Cluzel, 2007).

579 **Dolerite geochemistry and comparison with Poya Terrane Basalts**

580 Fifteen new representative samples of Early Eocene sills and dikes that crosscut the sediments
581 of Koné Facies and basalts of Poya Terrane have been analyzed for major, trace elements and REE at
582 the SARM-CRPG of Nancy France (for analytical procedure, accuracy and detection limits see online
583 supplementary material, Text S1 have been compared with those available in the literature regarding
584 basalts and dolerites of the Poya Terrane (Eissen et al, 1998; Cluzel et al, 2001; Audet, 2008).

585 All 42 dolerite samples in the data base have very similar sub alkaline basalt compositions
586 (46.8 ± 0.6 wt% SiO_2 ; 1.4 ± 0.2 wt% TiO_2 ; 14.1 ± 0.7 wt% Al_2O_3 ; 2.7 ± 0.4 wt% Na_2O ; 0.3 ± 0.1 wt% K_2O)
587 (online supplementary material, Table S3). Considering the relatively high water content (average 2.3
588 wt% H_2O) and erratic variation of some mobile elements, classification/discrimination based upon
589 “immobile” trace elements has been preferred. On the Zr/ TiO_2 vs. Nb/Y diagram (Pearce 1996),
590 which is considered a proxy of the classical TAS diagram of Le Bas et al (1986) for metamorphosed or
591 slightly altered rocks, all dolerite samples plot in a narrow area, on the high Nb/Y side of the basalt
592 field (Fig 8). In contrast, two sub-types may be identified on chondrite-normalized REE patterns
593 (Evensen et al., 1978; Pearce, 1982; Fig 9); i) LREE-depleted patterns ($(\text{La}/\text{Sm})_n = 0.91 \pm 0.06$; Fig 9a)
594 similar to the average N-MORB pattern (although their bulk REE content is two times higher; Gale et
595 al, 2013) only represent dikes that crosscut Poya Terrane basalts; and, ii) almost flat REE patterns
596 ($(\text{La}/\text{Yb})_n = 1.2 \pm 0.1$) without depletion in LREE ($(\text{La}/\text{Sm})_n = 1.00 \pm 0.20$; Fig 9b), some of which crosscut
597 Poya Terrane basalts, while the others represent sills in Kone Facies sediments. The former have
598 been generated from a slightly depleted shallow mantle source, and the latter are diagnostic of E-
599 MORBs (enriched MORBs), e.g. subalkaline basalts slightly enriched in LREE and LILE incompatible
600 elements with respect to “normal” MORB (N-MORB).

601 On the REE and trace elements expanded spider diagram normalized to the average N-MORB
602 (Fig. 10) (Sun and McDonough, 1989), patterns of dolerite dikes and sills of Poya and Kone facies are
603 all very similar, except two or three samples for which the zigzag pattern probably denotes some
604 analytical issue (incomplete leaching of some accessory minerals ?). A negative slope of LREE
605 depleted patterns (Fig. 10a) and undepleted patterns as well (Fig. 10b), and fractionation of LILE with
606 respect to HFSE are inconsistent with the MORB-like features of some dolerite samples and probably
607 signal some source heterogeneity, which may be due to near-ridge re-enrichment of the mantle
608 source, or source mixing (see discussion below).

609 Dolerite sills in the Kone Facies commonly display a weak Nb negative anomaly (Fig. 10b),
610 which is not present in E-MORB dikes crosscutting Poya basalts and is likely due to slight
611 contamination by wallrock terrigenous sedimentary rocks. The scarce occurrence of inherited older
612 zircons (~100 Ma) in some dolerites (online supplementary material, Data set S1) supports this
613 interpretation.

614 A single magmatic affinity is suggested by some incompatible trace element ratios, which are
615 considered to reflect source compositions and melting processes. On the Hf/3-Th-Ta triangular
616 diagram of Wood (1980) modified by Vermeesch (2006), E-MORB dolerites plot in a restricted area
617 similar to that of E-MORB flow and pillow basalts of the Poya Terrane (Fig 11). There is no difference
618 in Hf, Ta and Th ratios between LREE-depleted and LREE-undepleted dolerites, which therefore may
619 come from a mineralogically uniform source. Significantly, in contrast with dikes that crosscut Poya
620 Terrane basalts and have E-MORB and BABB features, the dolerites that intrude the Kone Facies
621 never display BABB signatures.

622 **Tectonic structure and metamorphism**

623 The Poya Terrane *sensu stricto* consists of hundreds of upright tectonic slices, a few meters to
624 a few hundred meters thick and a few tens of meters to several hundreds of meters long. In contrast,
625 sediments of the Kone Facies appear in much larger units, which can be followed laterally over
626 several km. The overall structure defined by sedimentary bedding and dolerite sills trends parallel to
627 the orientation of the island (NW-SE). However, it shows prominent variations due to gentle km-scale
628 folds with vertically plunging axes (Fig 1). Away from the basal thrust of the Peridotite Nappe, except
629 the numerous faults, the only noticeable tectonic structure at outcrop scale is meter-scale folds with
630 plunging axes homothetic to those of regional scale. Overall, these folds indicate a dextral shearing,
631 which is also a prominent late feature of the Eocene HP-LT metamorphic complex in the north of the
632 island (Maurizot et al, 1989; Cluzel et al, 2001), and does not appear in the overlying Peridotite
633 Nappe. In west coast units, schistosity only appears in sediment lenses in a zone about 100-200 m
634 thick beneath the basal thrust of the Peridotite Nappe and disappears downwards, it is roughly
635 parallel to lithologic boundaries whatever their dip. Asymmetrical boudinage of chert beds, S-C and
636 S-C-C' structures indicates top-to-the-SW sub-horizontal shearing consistent with the overall SW-
637 directed motion of the Peridotite Nappe.

638 The base of the Poya Terrane is rarely well exposed. However, where it can be observed on its
639 northeastern boundary, the underlying autochthonous sediments display a rough schistosity, steeply
640 dipping to the SW, without clear kinematic indications.

641 No evidence of metamorphism exists in Kone Facies rocks in the main west coast unit, except
642 for contact metamorphism in the vicinity of dolerite sills. Dolerites are also free of any ductile
643 deformation and recrystallization, even immediately beneath the Peridotite Nappe. Poya terrane
644 basalts display zeolite to lower greenschist facies due to hydrothermal alteration (ocean floor
645 metamorphism) and low grade burial metamorphism (Nicholson et al, 2000; Cluzel, 2001). In
646 contrast, in Hienghène and Touho areas (Fig 1) i.e, along the northeastern flank of the large
647 anticlinorium cored by Pouebo and Diahot HP-LT terranes (Fig. 2A), the east coast equivalents of
648 Poya Terrane basalts and Kone Facies are closely associated with tectonic lenses of serpentinized
649 peridotite and display evidence for polyphase recrystallization and deformation, which vanishes
650 southeastward. The earliest event is represented by contact metamorphism (recrystallization
651 spots/nodules) developed in Kone Facies turbidites close to dolerite sills (online supplementary
652 material, Fig. 5c). In turn, sediments and dolerites developed schistosity and experienced blueschist
653 facies metamorphism, now represented by scarce remains of blue amphibole in metadolerite (online
654 supplementary material, Fig. S4a & S4b). Finally, the whole set has been deformed by tight folds in
655 metasediments (online supplementary material, Fig. S5b) and due to higher strength, gentle folds in
656 metadolerite (online supplementary material, Fig. 5d). The folds trend N110°E on average, are
657 upright or slightly reclined to the south and crosscut by dextral faults with a similar trend. In
658 metadolerites, blueschist facies minerals have been extensively replaced/pseudomorphosed by a
659 lower amphibolite to greenschist facies association (green hornblende, tremolite-actinolite, chlorite).
660 The high-temperature schistosity is partly overprinted by spaced colder cataclasis. The polyphase
661 evolution of these units may be correlated with the major steps of the evolution of the HP-LT
662 complex; i) subduction, ii) exhumation and arching; and, iii) transcurrent (transpressive ?) dextral
663 faulting.

664 Discussion

665 The detrital sediments of the Kone Facies have the same provenance as the autochthonous
666 Formation à Charbon, e.g., mostly the underlying basement terranes, except for Cretaceous zircon
667 populations. The volcanoclastic character of some sandstones and importance of Coniacian-Santonian
668 detrital zircon populations of Kone Facies sediments, suggest greater proximity to volcanic centers
669 compared to the autochthonous Formation à Charbon. However, this is in contrast to the absence of
670 Late Cretaceous volcanic rocks in the Kone Facies. Nevertheless, it is worth noting that Kone Facies
671 rocks have no known basement and have been scrapped off the ancient passive margin. Thus, it is
672 possible that some Late Cretaceous syn-rift volcanic rocks have remained attached to the pre-Late
673 Cretaceous basement, and are not exposed at present. Alternatively, Late Cretaceous zircons may

674 have come from an as yet undiscovered Late Cretaceous volcanic arc, which could have been rifted
675 away eastward to form the basement of Loyalty or Fiji islands.

676 The upward and possibly lateral transition of sandstones into finer-grained turbidites and
677 finally pelagic argillites records Late Cretaceous deepening and progressive interruption of clastic
678 input due to post-rift submersion and thermal subsidence. This evolution is similar to that of
679 Formation à Charbon. Some differences exist however, because the latter accumulated in shallower
680 half-grabens and was followed by deposition of hemipelagic black cherts and micrites, which are not
681 present in the Kone facies. Instead, upward evolution towards bathyal siltstone and argillite suggest
682 that Kone facies sediments are intermediate between Formation à Charbon and bathyal argillite of
683 the Poya facies sensu stricto. Intermixing of distal turbidites and abyssal red argillite suggests that
684 Kone Facies sediments accumulated on the eastern passive margin of the Norfolk Ridge immediately
685 before and during oceanization of the South Loyalty Basin in Campanian time. From the origin of
686 Kone-Poya clastic sediments and abyssal rocks in the eastern passive margin of the Norfolk Ridge,
687 and occurrence of HP-LT minerals we infer that both belong to the lower plate of the
688 obduction/subduction system, thus reinforcing the accretion model.

689 The large difference that exists between strongly disrupted Poya Terrane basalts and Kone
690 Facies rocks, which form extensive units, suggests contrasting modes of tectonic emplacement.
691 Small-scale basalts and abyssal argillite slices have been peeled off the down-going plate and
692 accreted to the intra-oceanic Loyalty fore-arc. In contrast, rock units of the Kone Facies may result
693 from the tectonic inversion of the Late Cretaceous passive margin. They have been possibly detached
694 as one or several coherent units and thrust southwestward to their present location to the northeast
695 of Poya Terrane basalts.

696 The formation of a dolerite sill complex temporally correlates with subduction inception and
697 suggests some genetic link. However, there is a great difference between E-MORB sills of the lower
698 plate, and the various subduction-related dikes that crosscut the Peridotite Nappe (upper plate),
699 which are related to different processes.

700 E-MORBs are generally thought to form in off-axis seamounts and magma lenses a few km
701 away from the ridge (Han et al, 2014); they may also erupt at the ridge axis (Waters et al, 2011) and
702 are generally minor compared to N-MORB in “normal” oceanic basins. Alternatively, they may be an
703 important component of some marginal basins, especially those with multiple ridge junctions.
704 Formation of E-MORBs in the South Loyalty Basin is consistent with their appearance in modern
705 back-arc settings such as the North Fiji (Eissen et al, 1994) and Lau basins (Volpe et al, 1988). E-
706 MORBs may form by: i) mixing of shallow (depleted) and deeper (fertile) mantle sources (Waters et

707 al, 2011), ii) contamination of the asthenosphere by subducted OIB seamounts (Ulrich et al, 2012); or
708 alternatively iii) may result from two-stage partial melting of one single source (Donnelly et al, 2004).
709 EMORBs of the Poya Terrane have enriched geochemical and isotopic signatures and coexist with
710 BABBs coming from a depleted (N-MORB-like) source (Cluzel et al, 2001). Therefore the two-stage
711 melting model does not apply. The existence of a relatively wide range of isotopic compositions in E-
712 MORBS of the Poya Terrane ($2.5 < \epsilon_{Nd} < 6.6$) having the same trace element features (i.e. REE-Tr
713 patterns, Hf/Th; Fig 12) suggests source mixing or mantle heterogeneity as well.

714 Whatever the processes involved in their formation, eruption into the ancient passive margin of
715 E-MORBs with geochemical and isotopic signatures similar to those of the South Loyalty Basin itself
716 (Fig 11 and 12) ~25-30 My after the end of rift-related magmatism, represents a difficult issue.

717 Eruption of E-MORBs far away from the spreading ridge seems difficult unless they have been
718 horizontally channeled over long distances by lithosphere-scale faults, a process advocated under
719 some circumstances; e.g., in the Dead Sea Fault system (Weinstein and Garfunkel, 2014) or in parts
720 of the giant Central Atlantic Magmatic Province (Nomade et al, 2000). However, no evidence for such
721 a magma transfer appears in paleo-transform faults identified in the Peridotite Nappe of New
722 Caledonia.

723 Generating E-MORB out of a spreading ridge requires uplift of the asthenosphere that cannot be
724 achieved without prominent lithosphere thinning. A transcurrent regime could generate MORB-like
725 magmas within a narrow zone (pull apart) consistent with the location of Kone dolerites within the
726 ancient passive margin. However, mantle upwelling and partial melting would have first generated
727 deeper-sourced alkaline (OIB-like) magmas followed by shallower sub-alkaline MORB-like magmas.

728 Alternative scenarios involve evolution of the ancient spreading ridge after subduction inception
729 at or near the ridge at ca 56 Ma (Fig 13): i) either the ridge was subducted together with the lower
730 plate, then the partial melting zone should have generated similar melts (E-MORBs and BABBs) in the
731 upper plate and died out quickly by the effect of increasing pressure (Fig 12 b1) before being relayed
732 by incipient volcanic-arc activity (Fig 12 c1). However, Eocene E-MORBs and BABBs are absent in the
733 upper plate (the Peridotite Nappe) and this model does not apply. Alternatively, ii) the melt zone
734 may have remained at the same place by delamination of the lithosphere, swept the lower plate
735 continentward, and for a while, continued to generate E-MORB melts, which were erupted together
736 with prominent uplift (Fig 12 b2). This model is consistent with eruption of boninite-series magmas
737 directly over peridotites of the upper plate (Marchesi et al, 2009; Pirard et al, 2013; Cluzel et al, 2016;
738 Fig 12 c2). The second scenario, which fits well with the overall features of the Peridotite Nappe will

739 be preferred although ridge subduction is generally advocated in subduction inception models
740 (Gurnis et al, 2004 and references herein). It is worth noting that emplacement of E-MORB sill
741 complex was synchronous with temporary emersion of autochthonous units during the Late
742 Paleocene (Adio limestone; Maurizot, 2013), which records localized uplift of the Norfolk Ridge in
743 possible relation with its entry in the flexural fore-arc bulge. Alternatively, increase of compressional
744 stress may have occurred due to progressive subduction jamming by buoyant crust elements (Diahot
745 Terrane (Fig. 3). In addition to a fore-arc bulge, arching of the ancient Late Cretaceous margin may
746 have been enhanced by sub-plate heating by the almost extinct partial melting zone (see below).

747 Explaining why the EMORBs that intruded Kone Facies sediments have been emplaced as sills
748 instead of forming dikes is crucial for constraining the tectonic evolution of the Eocene
749 subduction/obduction complex. Sheeted sill complexes which occur in the oceanic crust, record an
750 imbalance between crustal extension and magma supply (Hopson, 2007). This is obviously the case in
751 Kone Facies rocks because extensional tectonism had already stopped since 25-30 My at the time of
752 intrusion, thus preventing magma ascent. However, the situation of the ancient Late Cretaceous
753 margin at the Paleocene-Eocene boundary was not that of an oceanic ridge.

754 Sills and laccoliths may also form in compressional settings (Kavanagh et al, 2006; Menand et al,
755 2010), and subduction of young and buoyant oceanic lithosphere generally results in horizontal
756 compressive stress, while the obliquity of the lower plate with respect to the trench generates an
757 oblique component to the convergence. In New Caledonia, transpression is recorded by the
758 occurrence at all scales of folds with steeply plunging axes, consistent with dextral transcurrent
759 tectonics, which are not present in autochthonous units or in the overlying Peridotite Nappe.
760 Therefore, it appears that accretion of oceanic crust and passive margin elements occurred during
761 dextral oblique subduction (Fig 3; Cluzel et al, 2001), which may have reactivated ancient structural
762 features of the passive margin. Active faulting may have channeled upward or horizontal magma
763 transit at depth, while at a shallower level, the decreasing lithospheric pressure favored vertical
764 tensile stress and enhanced formation of sill/laccoliths (Corry, 1988; Tibaldi et al, 2008).

765 A geodynamic model accounting for these new elements may be proposed. However, it is worth
766 noting that sketch cross sections of Fig. 14 cannot completely account for the evolution of the
767 eastern Norfolk margin, which at least during its last stages, developed in a transcurrent setting (Fig
768 3).

769

770 During the Coniacian and Santonian, extreme thinning of SE Gondwana margin generated
771 grabens/hemigrabens in which terrigenous sediments were deposited. Rifting was followed by

772 Campanian-Paleocene development of oceanic lithosphere and formation of a passive margin on
773 which deep-water turbidites accumulated, isolated several ribbons of continental crust, and
774 generated Poya Terrane basalts from a heterogeneous (BABB and EMORB) mantle source (Fig
775 14a&b).

776 In latest Paleocene-earliest Eocene time, shallow-dipping subduction started near the ridge and
777 inverted the basin. Poya Terrane basalts were obliquely accreted in the nascent Loyalty fore-arc. The
778 Loyalty fore-arc probably underwent uplift and erosion, leaving only deeply unroofed peridotites.
779 Meanwhile, the partial melt zone swept the base of the lower plate and generated dikes in the
780 marginal basin lithosphere and sills in the ancient passive margin. Localized uplift and emersion of
781 Norfolk Ridge may be correlated with this event (Fig 14c). Meanwhile, slab melts and ultra-depleted
782 magmas were generated in the mantle wedge and formed the Early Eocene dike set and boninite-
783 series fore-arc crust. When the ancient passive margin reached the convergence zone, Poya basalts
784 and Kone Facies were amalgamated and thrust together on autochthonous units (Fig 14d) where
785 they fed the mid to Late Eocene syntectonic basins. Finally, the whole set was thrust by (actually
786 subducted beneath) the Peridotite Nappe, which was again uplifted and eroded, preserving only
787 scarce remains (cumulates) of the fore-arc crust.

788

789 **Conclusion**

790 A reappraisal of the Poya Terrane based upon field data, sediment analysis, U-Pb zircon
791 geochronology, and whole-rock geochemistry has revealed that:

- 792 1. The extent of the main sedimentary component, referred to as Kone Facies, had been largely
793 underestimated and actually represents about one third of the bulk terrane surface.
- 794 2. These sediments are composed of sandstones and distal turbidites overlain by abyssal
795 argillites, which accumulated on the eastern passive margin of the Norfolk Ridge during
796 rifting and post-rift thermal subsidence.
- 797 3. Kone Facies sediments are about the same age as and of similar provenance as the
798 autochthonous Late Cretaceous Formation a Charbon, with a greater amount of detrital
799 zircon coming from contemporaneous magmatism.
- 800 4. Instead of derivation through the accretion of Late Cretaceous-Paleocene marginal basin
801 crust, the mafic magmatic component of Kone Facies formed as Early Eocene sills of E-MORB
802 affinity generated close to the time of subduction inception.
- 803 5. The predominance of E-MORBs over BABBs in the oceanic component of the Poya Terrane
804 should be reevaluated because fresher E-MORB dolerites have been oversampled.

- 805 6. At variance with previous interpretations, the lower plate (South Loyalty Basin) of the
806 subduction/obduction complex was probably of BABB affinity. This is consistent with the
807 composition of high-temperature amphibolites (metamorphic sole) and that of slab melts
808 intruded in the upper plate (the Peridotite Nappe).
- 809 7. Slices of Poya Terrane basalts were accreted at shallow depth in front of the Loyalty fore-arc.
810 In contrast, some elements were dragged down by tectonic erosion, subducted and formed
811 the Pouebo eclogitic mélange
- 812 8. The NE elements of the Poya Terrane (including Kone Facies) that crop out on the east coast
813 were subducted to depth sufficient for the development of blueschist facies metamorphism.
814 Together with involvement of passive margin sediments, this excludes any possibility that the
815 Poya Terrane originated from the upper plate (fore-arc) of the subduction-obduction system.
- 816 9. Late Oligocene reset of the U-Pb zircon system confirms the widespread occurrence of brittle
817 tectonics and hydrothermal activity contemporaneous with post-obduction granitoid
818 intrusion, which largely exceeds their area of occurrence in southern New Caledonia.

819

820 New Caledonia shows exceptional preservation of an example of subduction/obduction system,
821 which was not obscured by subsequent continent-continent collision. It appears that off-peeling of
822 the lower plate crust and accretion tectonics may generate large mafic allochthons, forming
823 disrupted bodies in suture zones. On a local scale, these mafic units are closely (within a few km)
824 associated with eclogites of similar composition that were exhumed through the subduction channel
825 independently of continental collision.

826

827

828 **Acknowledgements**

829 The travel and stay of MW in New Caledonia were partly funded by the international student
830 exchange program of the University of New Caledonia (UNC). The analytical work was supported by
831 the University of Tasmania and by funds gathered in the framework of UNC Continuous Training
832 Program. John Wakabayashi and Yildirim Dilek are thanked for extensive reviews and suggestions for
833 the improvement of the manuscript. Jay Thompson is thanked for his assistance in performing and
834 analyzing the zircon data. Warm thanks are due to the people of Netchaot for welcoming MW during
835 his field work and to Elisabeth for kindly lending her car.

836 Supporting information material is available online at [https://hal-insu.archives-ouvertes.fr/insu-](https://hal-insu.archives-ouvertes.fr/insu-01565604)
837 01565604

838

839

840 **References**

- 841 Adams C.J., Cluzel D., and Griffin W.L., 2009. Detrital zircon ages and provenance of sedimentary
842 rocks in basement Mesozoic terranes of New Caledonia. *Australian Journal of Earth Sciences* 56,
843 1023-1047. doi: 10.1080/08120090903246162
- 844 Adams C.J, Campbell H.J., Mortimer N. and Griffin W.L., 2013a The mid-Cretaceous transition from
845 basement to cover within sedimentary rocks in eastern New Zealand: evidence from detrital zircon
846 age patterns. *Geological Magazine* 150, 89-109. doi:10.1017/S0016756812000258
- 847 Adams C.J, Campbell H.J., Mortimer N. and Griffin W.L., 2013b. Detrital zircon geochronology and
848 sandstone provenance of basement Waipapa Terrane (Triassic–Cretaceous) and Cretaceous cover
849 rocks (Northland Allochthon and Houhora Complex) in northern North Island, New Zealand.
850 *Geological Magazine* 150, 3, 455-478. doi:10.1017/S0016756812000611
- 851 Adams C.J, Campbell H.J., Mortimer N. and Griffin W.L., 2016. Perspectives on Cretaceous Gondwana
852 break-up from detrital zircon provenance of southern Zealandia sandstones. *Geological Magazine*
853 doi:10.1017/S0016756816000285
- 854 Aitchison J., Clarke G., Cluzel D., and Meffre S., 1995a. Eocene arc-continent collision in New
855 Caledonia and implications for regional southwest Pacific tectonic evolution, *Geology*, 23, p. 161-
856 164.
- 857 Aitchison J.C., Meffre S. and Cluzel D., 1995b. Cretaceous/Tertiary radiolarians from New Caledonia,
858 *Geol. Soc. of New Zealand Miscellaneous Publ.* 81A, p. 70
- 859 Aitchison J.C., Ireland T.R., Clarke G.L., Cluzel D., Davis A.M. and Meffre S., 1998. Regional
860 implications of U/Pb SHRIMP age constraints on the tectonic evolution of New Caledonia,
861 *Tectonophysics* 299: 333-343. Audet, M.A., 2008. Le massif du Koniambo, Nouvelle-Calédonie:
862 formation et obduction d'un complexe ophiolitique du type SSZ. Enrichissement en nickel, cobalt et
863 scandium dans les profils résiduels. Unpubl. PhD thesis, University of New Caledonia, 327 p.
- 864 Avias J., 1967. Overthrust structure of the main ultrabasic New Caledonian massives. *Tectonophysics*,
865 4, 4-6, 531-541.
- 866 Baldwin S. L., Rawlings T. and Fitzgerald P.G., 2005. Thermochronology of the New Caledonian high-
867 pressure terrane: Implications for middle Tertiary plate boundary processes in the southwest Pacific.
868 *GSA Special publication*, 419, 117-134.

869 Ballance P.F. and Campbell J.D., 1993. The Murihiku arc-related basin of New Zealand (Triassic–
870 Jurassic). In: Ballance P. F. ed. South Pacific sedimentary basins (Sedimentary Basins of the World 2),
871 Elsevier, Amsterdam, 21–33.

872 Bryan S.E., Ewart A., Stephens C.J., Parianos J., and Downes P.J., 2000. The Whitsunday Volcanic
873 Province, Central Queensland, Australia: lithological and stratigraphic investigations of a silicic-
874 dominated large igneous province. *Journal of Volcanology and Geothermal Research* 99, 1-4, 55–78

875 Bryan S.E., Cook A.G., Allen C.M., Siegel C., Purdy D.J., Greentree J.S., and Uysal T., 2012. Early-mid
876 Cretaceous tectonic evolution of eastern Gondwana: from silicic LIP magmatism to continental
877 rupture. *Episodes*, 35 (1), 142-152.

878 Campbell, H.J. 1984. New records and taxa of Permian and Triassic fossils from New Caledonia and
879 New Zealand. *Alcheringa: Australasian Journal of Palaeontology*, 8, 151-167, doi:
880 10.1080/03115518408618940.

881 Campbell, H.J., Grant-Mackie, J.A. and Paris, J.P., 1985, Geology of the Moindou-Téremba area, New
882 Caledonia. Stratigraphy and structure of the Téremba Group (Permian -Lower Triassic) and Baie de St
883 Vincent Group (Upper Triassic–Lower Jurassic), *Géologie de la France*, 1, 19–36.

884 Campbell, H.J., Mortimer, N. and Raine, J.I., 2001. Geology of the Permian Kuriwao Group, Murihiku
885 Terrane, Southland, New Zealand. *New Zealand Journal of Geology and Geophysics*, 44, 485-500.

886 Carroué J. P., 1972. Carte et notice explicative de la carte géologique de la Nouvelle-Calédonie à
887 l'échelle du 1/50000: feuille Pouembout. Bureau de Recherches Géologiques et Minières, Orléans
888 France.

889 Carson, C.J., Powell R., Clarke G.L., 1999. Calculated mineral equilibria for eclogites in CaO-Na₂O-FeO-
890 MgO-Al₂O₃-SiO₂-H₂O: application to the Pouebo Terrane, Pam Peninsula, New Caledonia. *Journal of*
891 *Metamorphic Geology*, 17, 9-24.

892 Chardon D., Austin Jr. J. A., Cabioch G., Pelletier B., Sastrup S., and Sage F., 2008. Neogene history of
893 the northeastern New Caledonia continental margin from multichannel reflection seismic profiles.
894 *Comptes Rendus Geoscience* 340, 68–73. doi:10.1016/j.crte.2007.09.017
895 Clarke G., Aitchison J.C., and
896 Cluzel D., 1997. Eclogites and blueschists of the Pam Peninsula, NE New Caledonia: a reappraisal.
Journal of Petrology 38, 7, 843-876.

897 Cluzel D., Aitchison J.C., Clarke G., Meffre S. and Picard C., 1994. Point de vue sur l'évolution
898 tectonique et géodynamique de la Nouvelle-Calédonie, Comptes Rendus Académie des Sciences
899 Paris. 319, 6, 683-688.

900 Cluzel D., Picard C., Aitchison J., Laporte C., Meffre S. and Parat F., 1997. La Nappe de Poya (ex-
901 Formation des basaltes) de Nouvelle-Calédonie (Pacifique SW), un plateau océanique Campanien-
902 Paléocène supérieur obducté à l'Eocène supérieur. Comptes Rendus Académie des Sciences Paris.
903 324, 443-451.

904 Cluzel D., 1998. Le "flysch post-obduction" de Népoui, un bassin transporté ? Conséquences sur l'âge
905 et les modalités de l'obduction tertiaire en Nouvelle-Calédonie (Pacifique sud-ouest) Comptes
906 Rendus Académie des Sciences Paris., 327: 419-424

907 Cluzel D., Chiron D. and Courme M.D., 1998. Discordance de l'Eocène supérieur et événements pré-
908 obduction en Nouvelle-Calédonie (Pacifique sud-ouest) Comptes Rendus Académie des
909 Sciences Paris., 327: 485-91

910 Cluzel D., Aitchison J.C., and Picard C., 2001. Tectonic accretion and underplating of mafic terranes in
911 the Late Eocene intraoceanic fore-arc of New Caledonia (Southwest Pacific). Geodynamic
912 implications. Tectonophysics 340, 1-2, 23-60.

913 Cluzel D., and Meffre S., 2002. L'unité de la Boghen (Nouvelle-Calédonie, Pacifique sud-ouest): un
914 complexe d'accrétion jurassique. Données radiochronologiques préliminaires U-Pb sur les zircons
915 détritiques. Comptes Rendus Géosciences. 334, 867-874.

916 Cluzel D., Bosch D., Paquette J.L., Lemennicier Y., Montjoie Ph, and Ménot R.P., 2005. Late Oligocene
917 post-obduction granitoids of New Caledonia: a case for reactivated subduction and slab break-off.
918 The Island Arc, 14, 254-271.

919 Cluzel D., Meffre S., Maurizot P., and Crawford A.J., 2006. Earliest Eocene (53 Ma) convergence in the
920 Southwest Pacific; evidence from pre-obduction dikes in the ophiolite of New Caledonia. Terra Nova
921 18, 395-402.

922 Cluzel D., Adams C.J., Meffre S., Campbell H., and Maurizot P., 2010. Discovery of Early Cretaceous
923 rocks in New Caledonia (Southwest Pacific). New geochemical and U-Pb zircon age constraints on the
924 transition from subduction to marginal breakup. The Journal of Geology 118, 4, 381-397.

925 Cluzel D., Adams C.J., Maurizot P., and Meffre S., 2011. Detrital zircon records of Late Cretaceous syn-
926 rift sedimentary sequences of New Caledonia: an Australian provenance questioned. *Tectonophysics*
927 501, 1-4, 17-27. doi: 10.1016/j.tecto.2011.01.007

928 Cluzel D., Jourdan F., Meffre S., Maurizot P., and Lesimple S., 2012a. The metamorphic sole of New
929 Caledonia ophiolite; $^{40}\text{Ar}/^{39}\text{Ar}$, U-Pb, and geochemical evidence for subduction inception at a
930 spreading ridge. *Tectonics*. 31, 3, doi:10.1029/2011TC003085, 2012.

931 Cluzel D., Maurizot P., Collot J. and Sevin B., 2012b. An outline of the Geology of New Caledonia;
932 from Permian-Mesozoic Southeast-Gondwanaland active margin to Tertiary obduction and
933 supergene evolution. *Episodes* 35, 1, 72-86.

934 Cluzel D., Ulrich M., Jourdan F., Paquette J.L., Audet M.A., Secchiari A., and Maurizot P., 2016. Early
935 Eocene clinoenstatite boninite and boninite-series dikes of the ophiolite of New Caledonia; a witness
936 of slab-melt enrichment of the mantle wedge in a nascent volcanic arc. *Lithos*; doi:
937 10.1016/j.lithos.2016.04.031

938 Corry, C.E., 1988. Laccoliths mechanics of emplacement and growth. *Geological Society of America*
939 *Special Paper* 220, 116p.

940 Crampton J., Mumme T., Raine I., Roncaglia L., Schiøler P., Strong P., Turner G., and Wilson G., 2000.
941 Revision of the Piripauan and Haumurian local stages and correlation of the Santonian-Maastrichtian
942 (Late Cretaceous) in New Zealand. *New Zealand Journal of Geology and Geophysics* 43, 309-333

943 Crawford A.J., Meffre S., and Symonds P.A., 2003. 120 to 0 Ma tectonic evolution of the Southwest
944 Pacific and analogous geological evolution of the 600 to 220 Ma Tasman Fold Belt System. *Geological*
945 *Society of Australia, Special Publication* 22, 377-397.

946 Dickinson, W.R., 1970. Interpreting detrital modes of greywacke and arkose, *Journal of Sedimentary*
947 *Petrology*, 40, 695-707.

948 Dilek, Y., 2003. Ophiolite concept and its evolution, in Dilek, Y., and Newcomb, S., eds., *Ophiolite*
949 *concept and the evolution of geological thought: Boulder, Colorado*, Geological Society of America
950 *Special Paper* 373, p. 1–16. Donnelly, K. E., Goldstein, S. L., Langmuir, C. H. and Spiegelman, M., 2004.
951 Origin of enriched ocean ridge basalts and implications for mantle dynamics. *Earth and Planetary*
952 *Science Letters* 226, 347-366.

953 Eissen, J.P., Nohara, M., Cotten, J., and Hirose, K., 1994. The North Fiji Basin basalts and their
954 magmatic sources: I. Incompatible elements constraints. *Marine Geology* 116, 163– 178.

955 Eissen, J.P., Crawford, A.J., Cotten J., Meffre S., Bellon H., and Delaune M., 1998. Geochemistry and
956 tectonic significance of basalts in the Poya Terrane, New Caledonia. *Tectonophysics*, 284, 203-219.

957 Evensen, N.M., Hamilton, P.J. and O'Nions, R. K., 1978. Rare earth abundance in chondritic
958 meteorites. *Geochim. Cosmochim. Acta*, 42, 1199-212. Gale A., C. A. Dalton, C. H. Langmuir, Y. Su, and
959 J.-G. Schilling (2013), The mean composition of ocean ridge basalts, *Geochemistry Geophysics*
960 *Geosystems*, 14, 489–518, doi:10.1029/2012GC004334.

961 Gautier P., Quesnel B., Boulvais Ph. and Cathelineau M., 2016. The emplacement of the Peridotite
962 Nappe of New Caledonia and its bearing on the tectonics of obduction. *Tectonics* 35, 12, 3070–3094.
963 doi:10.1002/2016TC004318.

964 Gazzi, P., 1966. Le arenarie del flysch sopracretaceo dell'Appennino modenese; correlazioni con il
965 flysch di Monghidoro: *Mineralogica e Petrografica Acta*, 12, 69-97.

966 Grant-Mackie J. A., Paris J.P., Freinex S., and Campbell. H.J., 1977. Advances in correlation of
967 Mesozoic sequence of New Zealand and New Caledonia. 25th International Geological Congress,
968 Abstract Volume, 268-269. Sydney 1976.

969 Guillon, J.-H., and Gonord. H., 1972. Premières données radiométriques concernant les basaltes de
970 Nouvelle-Calédonie. Leurs relations avec les grands événements de l'histoire géologique de l'arc
971 mélanésien interne au Cénozoïque. *Comptes Rendus Academie des Sciences Paris, Ser. D.*, 275, 309-
972 312.

973 Gurnis, M., Hall C., and Lavier L., 2004. Evolving force balance during incipient subduction,
974 *Geochemistry Geophysics Geosystems*, 5, Q07001, doi:10.1029/2003GC000681.

975 Han S., Carbotte S.M., Carton H., Mutter J.C., Aghaei O., Nedimovic M.R., and Canales P.J., 2014.
976 Architecture of on-and off-axis magma bodies at EPR 9°37-40'N and implications for oceanic crustal
977 accretion. *Earth and Planetary Science Letters* 390, 31–44

978 Harries, P.J., Kauffman, E.G., Crampton, J.S. (Redacteurs), Bengtson, P., Cech, S., Crame, J.A., Dhondt,
979 A.V., Ernst, G., Hilbrecht, H., Lopez, Mortimore, G.R., Tröger, K.-A., Walaszczyk, I. and Wood, C.J. 1996.
980 *Mitteilungen aus dem Geologisch - Paläontologischen Museum der Universität Hamburg*, 77: 641-
981 671.

982 Hayes D. E., and Ringis J., 1973. Seafloor spreading in the Tasman Sea, *Nature (London)*, 244(5408),
983 454-458.

984 Hopson C.A. 2007. Subvolcanic sills and non-sheeted dikes in ophiolites: Occurrence, origin, and
985 tectonic significance for oceanic crust generation. Geological Society of America Special Papers 419,
986 225-254. doi: 10.1130/2006.2419(12)

987 Kavanagh JL, Menand T., and Sparks R.S.J., 2006. An experimental investigation of sill formation and
988 propagation in layered elastic media. Earth and Planetary Science Letters 245 (3), 799-813

989 Lagabrielle Y., Chauvet A., Ulrich M. and Guillot S., 2013. Passive obduction and gravity-driven
990 emplacement of large ophiolitic sheets: The New Caledonia ophiolite (SW Pacific) as a case study?
991 Bulletin de la Société Géologique de France, 184, 6, 545-556

992 Le Bas M. J., Le Maitre R. W., Streickeisen A., Zanettin B., and IUGS Subcommittee on the
993 Systematics of Igneous Rocks, 1986. A Chemical Classification of Volcanic Rocks Based on the Total
994 Alkali-Silica Diagram. Journal of Petrology 27 (3): 745-750 doi:10.1093/petrology/27.3.745

995 Leblanc M., 1995. Chromitite and ultramafic rock compositional zoning through a paleo-transform
996 fault, Poum, New Caledonia. Economic Geology and the Bulletin of the Society of Economic
997 Geologists, 90, 7, 2028-2039

998 Ludwig, K.R., 2012. User's Manual for Isoplot 3.75; a Geochronological Toolkit for Microsoft Excel.
999 Berkeley Geochronology Center Special Publication No. 5, 75 p.

1000 Marchesi C., Garrido C.J., Godard M., Belley F., and Ferré E., 2009. Migration and accumulation of
1001 ultra-depleted subduction-related melts in the Massif du Sud ophiolite (New Caledonia). Chemical
1002 Geology 266, 171-186.

1003 Maurizot P., Eberlé J.M., Habault C., and Tessarolo C., 1989. Carte géol. Territoires d'Outre-Mer,
1004 Nouvelle-Calédonie (1/50 000), feuille Pam-Ouégoa, 2e édition, B.R.G.M., Notice explicative par
1005 Maurizot P., Eberlé J.M., Habault C., Tessarolo C., 81 pp.

1006 Maurizot P. and Vendé-Leclerc M., 2009. 1:500,000 Geological map of New Caledonia, Service
1007 Géologique de la Nouvelle-Calédonie (Geological Survey), Government of New Caledonia
1008 (www.georep.nc)

1009 Maurizot, P. 2011. First sedimentary record of the pre-obduction convergence in New Caledonia :
1010 formation of an Early Eocene accretionary complex in the north of Grande Terre and emplacement of
1011 the ' Montagnes Blanches ' nappe. Bulletin de la Société Géologique de France, 182, 6, 479-491.

- 1012 Maurizot P., 2013. Palaeocene age for the Adio Limestone, New Caledonia: stratigraphic and regional
1013 context. *New Zealand Journal of Geology and Geophysics*, 56, 1, 16-26.
1014 <http://dx.doi.org/10.1080/00288306.2012.735677>
- 1015 McBride, E.F., 1989. Quartz cement in sandstones: a review, *Earth Science Reviews*, 26 (1-3), 69-112.
- 1016 Meffre, S., 1995. The development of island-arc related ophiolites and sedimentary sequences in
1017 New Caledonia. Ph D. thesis, University of Sydney, 258 pp.
- 1018 Meffre, S., Aitchison, J.C. and Crawford, A.J. 1996. Geochemical evolution and tectonic significance of
1019 boninites and tholeiites from the Koh Ophiolite, New Caledonia. *Tectonics*, 15, 67-83.
- 1020 Menand, T., Daniels K. A., and Benghiat P., 2010. Dyke propagation and sill formation in a
1021 compressive tectonic environment, *Journal of Geophysical Research*, 115, B08201,
1022 doi:10.1029/2009JB006791.
- 1023 Mortimer, N., Gans, P.B., Palin, J.M. and Herzer, R.H. 2014. Eocene and Oligocene basins and ridges
1024 of the Coral Sea-New Caledonia region: tectonic link between Melanesia, Fiji and Zealandia.
1025 *Tectonics*, 33, doi: 10.1002/2014TC003598.
- 1026 Nicholson K.N., Picard C., and Black P.M., 2000, A comparative study of Late Cretaceous ophiolitic
1027 basalts from New Zealand and New Caledonia : implications for the tectonic evolution of the SW
1028 Pacific. *Tectonophysics* 327, 157-171.
- 1029 Nomade S., Théveniaut H., Chen Y., Pouclet A., and Rigollet C., 2000. Paleomagnetic study of French
1030 Guyana Early Jurassic dolerites: hypothesis of a multistage magmatic event. *Earth and Planetary
1031 Science Letters* 184, 1, 155-168. doi: 10.1016/S0012-821X(00)00305-8
- 1032 Paquette J.L. and Cluzel D., 2007. U–Pb zircon dating of post-obduction volcanic-arc granitoids and a
1033 granulite-facies xenolith from New Caledonia. Inference on Southwest Pacific geodynamic models.
1034 *International Journal of Earth Sciences (Geologisches Rundschau)* 96, 613–622. doi: 10.1007/s00531-
1035 006-0127-1
- 1036 Paris J.P., Andreieff P., Coudray J., 1979. Sur l'âge éocène supérieur de la mise en place de la nappe
1037 ophiolitique de NouvelleCalédonie déduit d'observations nouvelles sur la série de Népoui. *C.R. Acad.
1038 Sci. Fr., série D*, 288, 1659-1661.
- 1039 Paris, J.P. 1981. *Géologie de la Nouvelle-Calédonie*. Mémoire du Bureau de Recherche Géologique et
1040 Minière, 113, 279 pp.

1041 Pearce, J.A., 1982. Trace element characteristics of lavas from destructive plate margins. In Thorpe
1042 R.S. (Ed) *Andesites*, Wiley, Winchester, 525-548.

1043 Pearce, J. A., 1996. A users guide to basalt discrimination diagrams. In: Wyman, D. A. (Eds) *Trace
1044 Element Geochemistry of Volcanic Rocks: Applications for Massive Sulphide Exploration*. Geological
1045 Association of Canada, Short Course Notes 12, 79-113.

1046 Pirard C., Hermann J., and O'Neill H., 2013. Petrology and geochemistry of the crust-mantle boundary
1047 in a nascent arc, Massif du Sud Ophiolite, New Caledonia, SW Pacific. *Journal of Petrology* 54 (9),
1048 1759-1792. doi: 10.1093/petrology/egt030

1049 Pirard C. and Spandler C., 2017. The zircon record of high-pressure metasedimentary rocks of New
1050 Caledonia: Implications for regional tectonics of the south-west Pacific. *Gondwana Research*, 46, 79-
1051 94. doi: 10.1016/j.gr.2017.03.001

1052 Prinzhofer A., and Nicolas A., 1980. The Bogota peninsula, New
1053 Caledonia: a possible oceanic transform fault. *Journal of Geology* 88, 387-398

1054 Prinzhofer, A., and Allègre, C.J., 1985. Residual peridotites and the mechanisms of partial melting.
1055 *Earth and Planetary Science Letters* 74, 251–265.

1056 Prinzhofer, A., 1987. Structure et pétrologie d'un cortège ophiolitique: le massif du Sud (Nouvelle-
1057 Calédonie), Thèse Ingénieur-Docteur de l'Ecole Nationale Supérieure du Pétrole et des Moteurs,
1058 University Paris VII, 244 pp.

1059 Quesnel, B., Gautier, P., Cathelineau, M., Boulvais, P., Couteau, C. and Drouillet, M. 2016. The
1060 internal deformation of the Peridotite Nappe of New Caledonia: a structural study of serpentine-
1061 bearing faults and shear zones in the Koniambo Massif. *Journal of Structural Geology*, 85, 51-67, doi:
10.1016/j.jsg.2016.02.006.

1062 Schilling, J.G., Zajac, M., Evans, R., Johnston, T., White, W., Devine, J.D. and Kingsley, R., 1983.
1063 Petrologic and geochemical variations along the Mid-Atlantic Ridge from 29 degrees N to 73 degrees
1064 N. *American Journal of Science*, 283(6), 510-586.

1065 Secchiari A., Montanini A., Bosch D., Macera P. and Cluzel D., 2016. Melt extraction and enrichment
1066 processes in the New Caledonia Iherzolites: evidence from geochemical and Sr-Nd isotope data.
1067 *Lithos* 260, 28–43. doi: 10.1016/j.lithos.2016.04.030

1068 Spandler C., Rubatto D. and Hermann, J., 2005, Late Cretaceous-Tertiary tectonics of the southwest
1069 Pacific: Insights from U-Pb sensitive, high resolution ion microprobe (SHRIMP) dating of eclogite
1070 facies rocks from New Caledonia: *Tectonics*, v. 24, TC3003. doi:10.1029/2004TC001709

1071 Sun, S. S., and McDonough W. I., 1989. Chemical and isotopic systematics of oceanic basalts:
1072 Implications for mantle composition and processes, in *Magmatism in the Ocean Basins*, edited by A.
1073 D. Saunders and M. D. Norry, Geological Society Special Publication 42, 313–345.

1074 Tibaldi A., Vezzoli L., Pasquare F. A., and Rust D., 2008. Strike-slip fault tectonics and the
1075 emplacement of sheet-laccolith systems: The Thverfell case study (SW Iceland). *Journal of Structural*
1076 *Geology* 30, 274-290

1077 Titus S.J., Maes S.M., Benford B., Ferré E.C., and Tikoff B., 2011. Fabric development in the mantle
1078 section of a paleotransform fault and its effect on ophiolite obduction, New Caledonia. *Lithosphere* 3,
1079 3, 221-244. doi: 10.1130/L122.1

1080 Tröger K.-A., 2000. Upper Cretaceous Inoceramids of Europe. *Memoir of the Geological Society of*
1081 *India*. 46, 119–130

1082 Ulrich M., Picard C., Guillot S., Chauvel C., Cluzel D., and Meffre S. 2010. Multiple melting stages and
1083 refertilization as indicators for ridge to subduction formation: the New Caledonia Ophiolite. *Lithos*
1084 115, 223-236. doi:10.1016/j.lithos.2009.12.011

1085 Ulrich, M., Hémond C., Nonnotte P., and Jochum K. P., 2012. OIB/seamount recycling as a possible
1086 process for E-MORB genesis. *Geochemistry Geophysics Geosystems*, 13, Q0AC19,
1087 doi:10.1029/2012GC004078

1088 Vermeesch P., 2006. Tectonic discrimination diagrams revisited. *Geochemistry, Geophysics,*
1089 *Geosystems* 7, 6, Q06017, doi: 10.1029/2005GC001092

1090 Vitale Brovarone, A., and Agard, P., 2013. True metamorphic isograds or tectonically sliced
1091 metamorphic sequence? New high-spatial resolution petrological data for the New Caledonia case
1092 study. *Contributions to Mineralogy and Petrology* 166, 2, 451.

1093 Volpe A.M., MacDougall J.D., and Hawkins J.M., 1988. Lau Basin basalts (LBB): trace elements and Sr-
1094 Nd isotopic evidence for heterogeneity in back-arc basin mantle. *Earth and Planetary Science Letters*
1095 90, 174-186.

1096 Wakabayashi, J. and Dilek, Y. 2000. Spatial and temporal relations between ophiolites and their
1097 subophiolitic soles: a test of models of forearc ophiolite genesis, In: Dilek, Y., Moores, E.M., Elthon, D.
1098 and Nicolas, A. (eds) *Ophiolites and Oceanic Crust: New Insights from Field Studies and the Ocean*
1099 *Drilling Program*. Geological Society of America, Special Papers, 349, 53-64.

1100 Waters C.L., Sims K.W.W., Perfit M.R., Blichert-Toft J., and Blusztajn J., 2011. Perspective on the
1101 Genesis of E-MORB from Chemical and Isotopic Heterogeneity at 9-10°N East Pacific Rise. *Journal of*
1102 *Petrology* 52, 3 565-602. doi:10.1093/petrology/egq091

1103 Weinstein Y. and Garfunkel Z., 2014. The Dead Sea Transform and the Volcanism in Northwestern
1104 Arabia. In: Garfunkel Z. et al. (eds.), *Dead Sea Transform Fault System: Reviews. Modern Approaches*
1105 *in Solid Earth Sciences* 6, 91-108. Springer Science+Business Media Dordrecht doi: 10.1007/978-94-
1106 017-8872-4_4

1107 Whitten M., 2015. Formation de Koné: Recording the final stages of Gondwana breakup in New
1108 Caledonia. Hons Thesis, University of Tasmania, 41p.

1109 Wood, D. A. 1980. The application of a Th-Hf-Ta diagram to problems of tectonomagmatic
1110 classification and to establishing the nature of crustal contamination of basaltic lavas of the British
1111 Tertiary volcanic province. *Earth and Planetary Science Letters* 50, 11–30.

1112

1113 **Figure captions**

1114 Figure 1: Geological sketch map of New Caledonia

1115 Figure 2: sketch cross sections of New Caledonia to show the relationships between the divers
1116 alochthonous units, HP-LT metamorphic complex, HT amphibolites (metamorphic sole) and post-
1117 obduction granitoids.

1118 Figure 3: a model for the tectonic evolution of the Loyalty Arc from Paleocene subduction inception
1119 to late Eocene obduction and subduction blocking (after Cluzel et al, 2001).

1120 Figure 4: Ternary plot of Koné sandstones displaying the relative amount of quartz, feldspars
1121 (plagioclase and potassium feldspar) and lithic clasts, using the Gazzi (1966) and Dickinson (1970)
1122 method of point counting. Figure 5: comparison of Cretaceous detrital zircon age populations to show
1123 the prominent importance of Coniacian-Santonian (synchronous) zircon population in Kone Facies
1124 compared to Fm. a Charbon (online supplementary material, Data set S1).

1125 Figure 6: Paleozoic-Proterozoic detrital zircon age populations of the Late Cretaceous Fm.à Charbon
1126 and Kone Facies (online supplementary material, Data set S1).

1127 Figure 7: 7a: U-Pb microzircon dating of representative dolerite of the Kone Facies (Koné quarry,
1128 west coast); 7b: cluster around 54.4 Ma of U-Pb microzircon ages of dolerites sills intruded in Kone
1129 Facies sediments (online supplementary material, Data set S2); 7c: U-Pb microzircon dating of
1130 dolerite of the Kone Facies from the Thiem Unit (east coast); 7d: partial reset of U-Pb microzircon
1131 ages of a sheared dolerite of the Thiem Unit to suggest Late Oligocene overprint.

1132 Figure 8: Zr/TiO₂ vs. Nb/Y classification diagram for weathered or metamorphic rocks (Pearce, 1996)
1133 to show dolerites compositions that dominantly plot in the field of subalkaline basalts

1134 Figure 9: REE diagram of Early Eocene dolerites normalized to the chondrite C1 (Evensen et al, 1978).
1135 9a: LREE-depleted dolerites in Poya Terrane and Kone Facies; 9b: flat REE patterns of E-MORBs
1136 dolerites

1137 Figure 10: REE and Trace elements spiderdiagram of dolerites normalized to the N-MORB (Pearce,
1138 1982). 10a: LREE-depleted patterns; 10b LREE undepleted patterns showing minor Nb negative
1139 anomaly possibly due to contamination by host rock.

1140 Figure 11: Hf/3-Th-Ta ternary diagram of Wood (1980) modified by Vermeesch (2006) to compare
1141 discriminant trace elements ratios of Poya Terrane basalts (BABB and E-MORBs) and dolerite sills and
1142 dikes that crosscut both Poya and Kone Facies rocks.

1143 Figure 12: EpsNd vs Hf/Th diagram to show variable ϵNd ratios of E-MORB dolerites with similar
1144 trace-elements ratios, thus suggesting source mixing. Data with white symbols are from Cluzel et al
1145 (2011); data with plain symbols are from this study (E-MORB sills from Kone Facies; online
1146 supplementary material, Table S4).

1147 Figure 13: Two possible scenarios for the inception of Early Eocene subduction: Fig. 14b1 and 14c1
1148 subduction of the partial melting zone (ridge) and eruption of EMORB in the upper plate; Fig 14b2
1149 and 14c2 preferred scenario with EMORB erupted in the lower plate

1150 Figure 14: Geodynamic model for the evolution of Poya Terrane from subduction inception to
1151 obduction

1152

Figure 1.

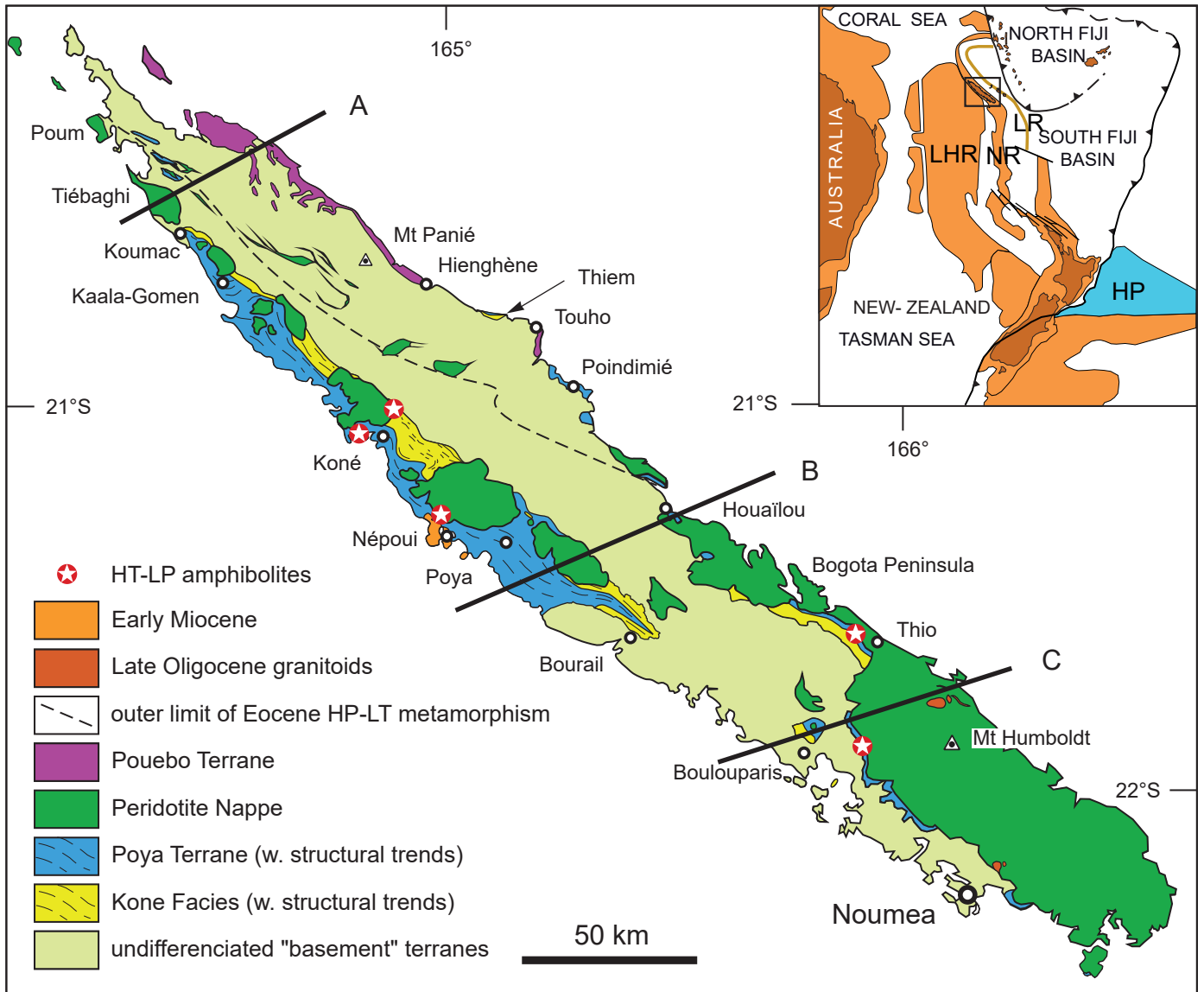


Figure 2.

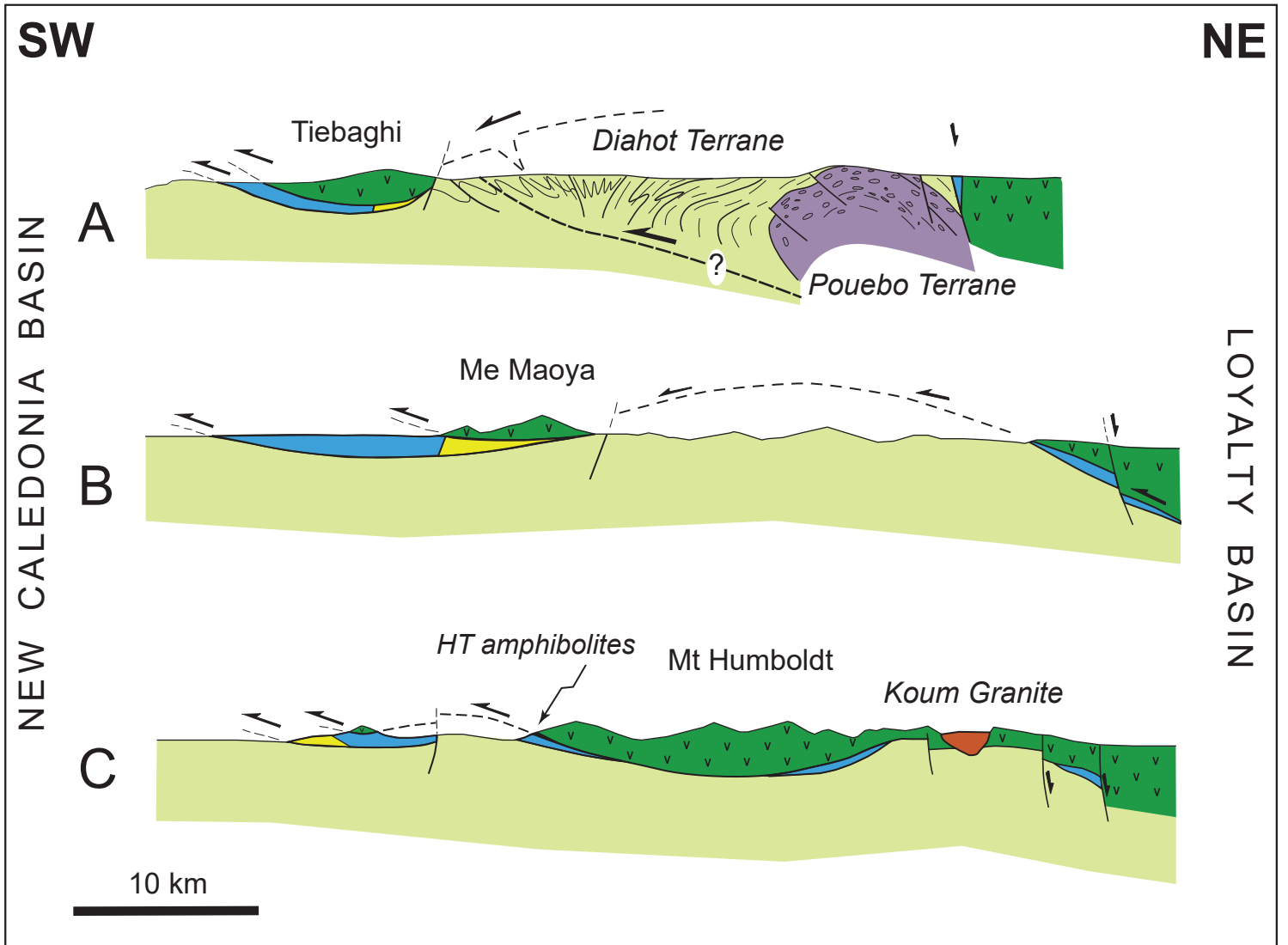
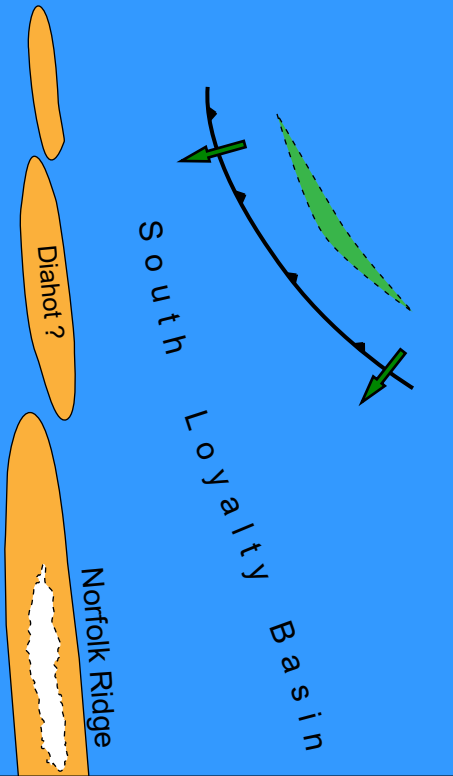
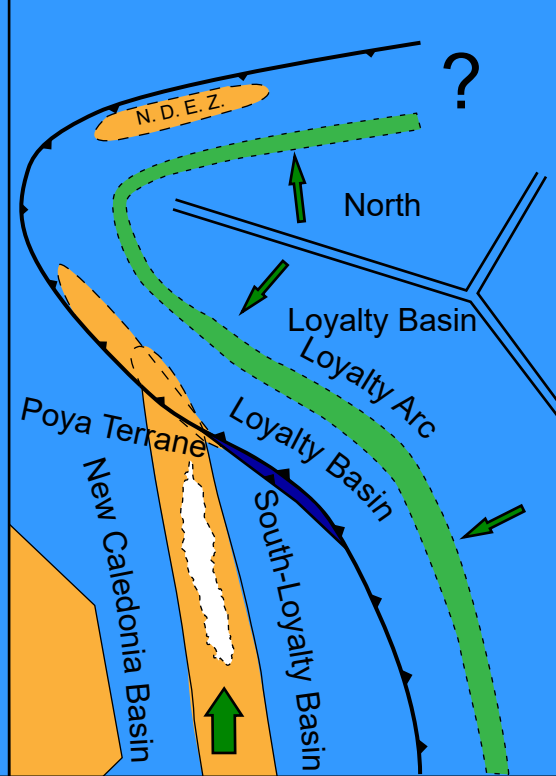


Figure 3.

Earliest Eocene (55 Ma)



Bartonian (38 Ma)



Oligocene (30 Ma)

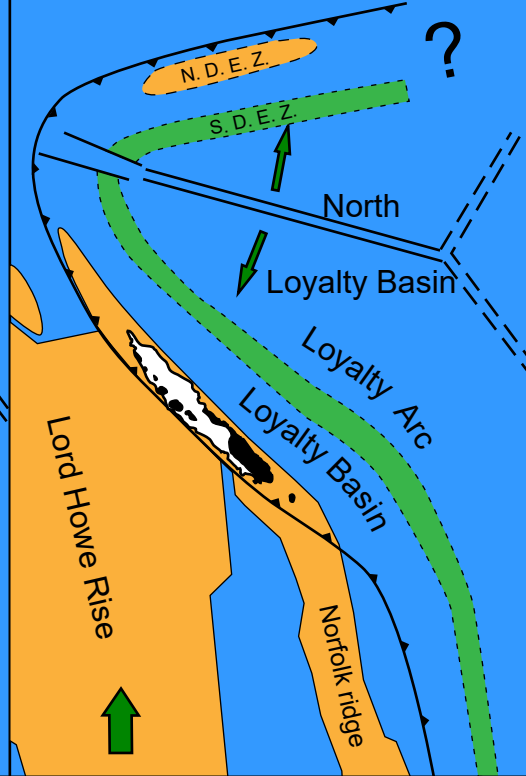


Figure 4.

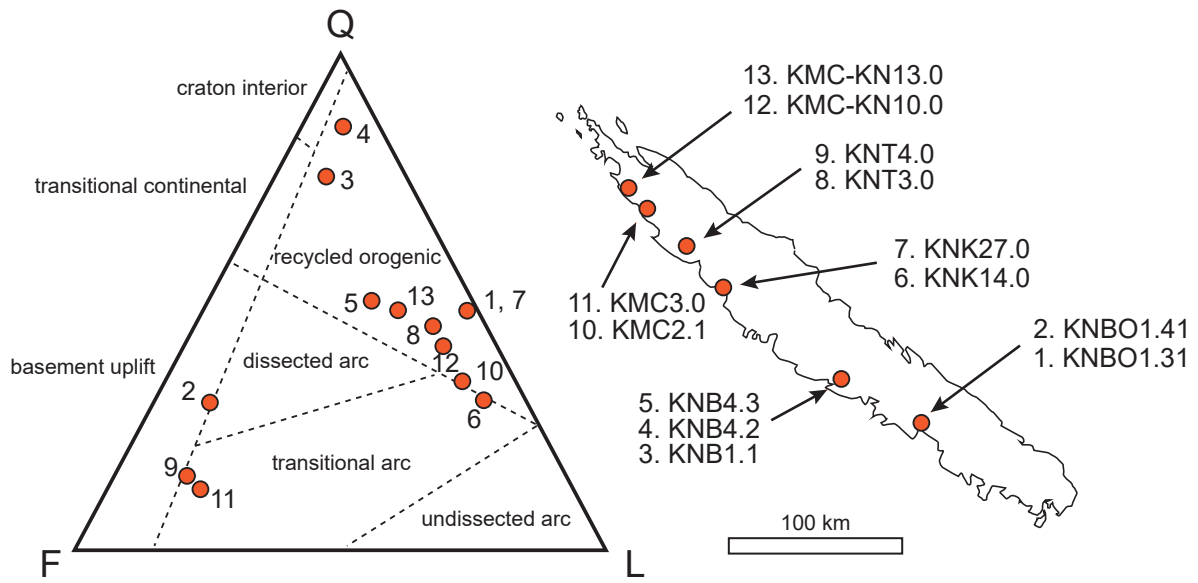


Figure 5.

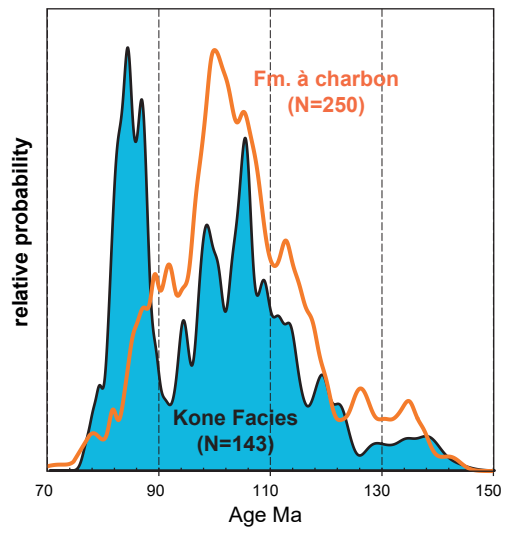


Figure 6.

Relative probability

Kone Facies

200 300 400 500 600 700 800 900 1000 1100 1200 1300 1400 1500
Age Ma

Relative probability

Fm. a charbon

200 300 400 500 600 700 800 900 1000 1100 1200 1300 1400 1500
Age Ma

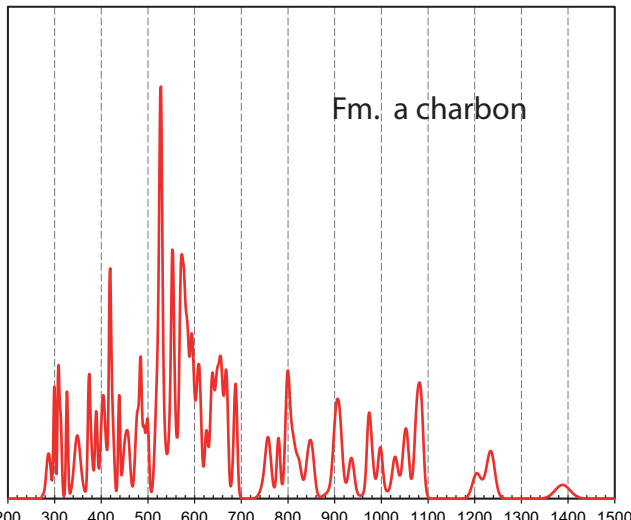
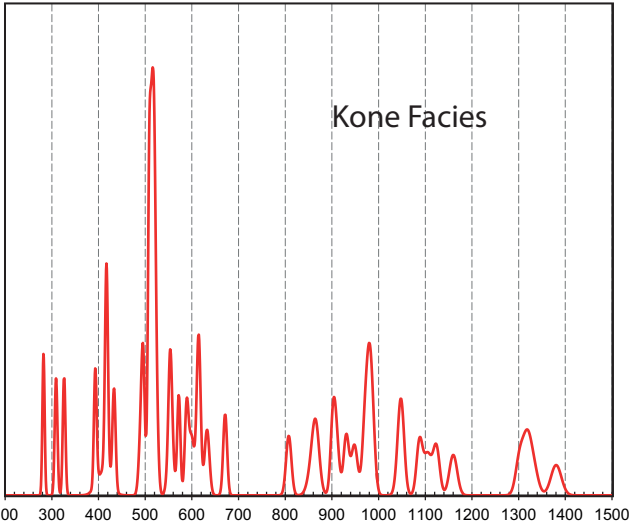


Figure 7.

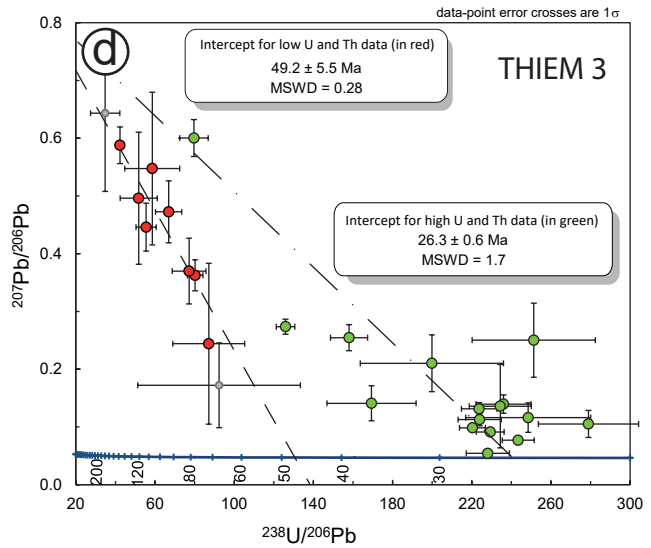
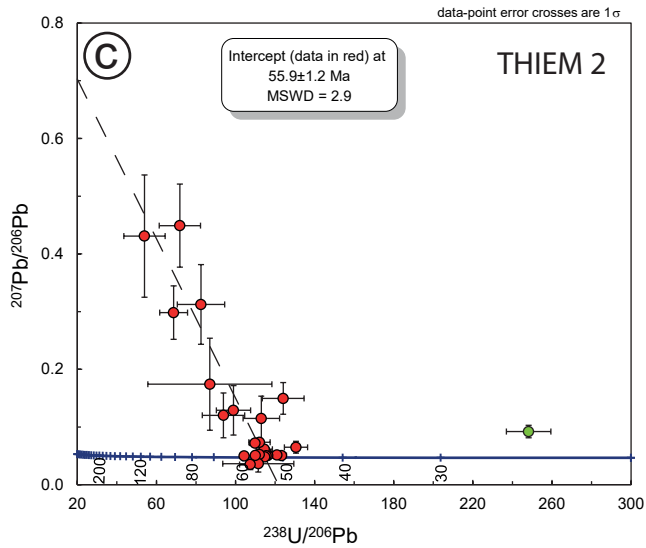
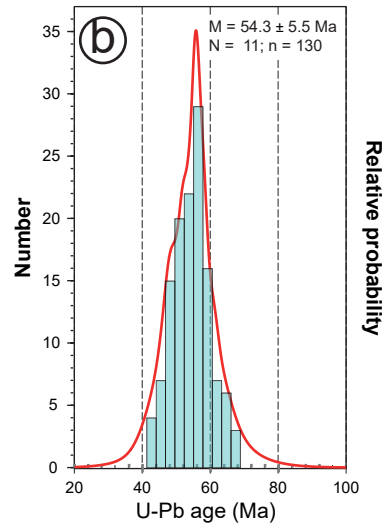
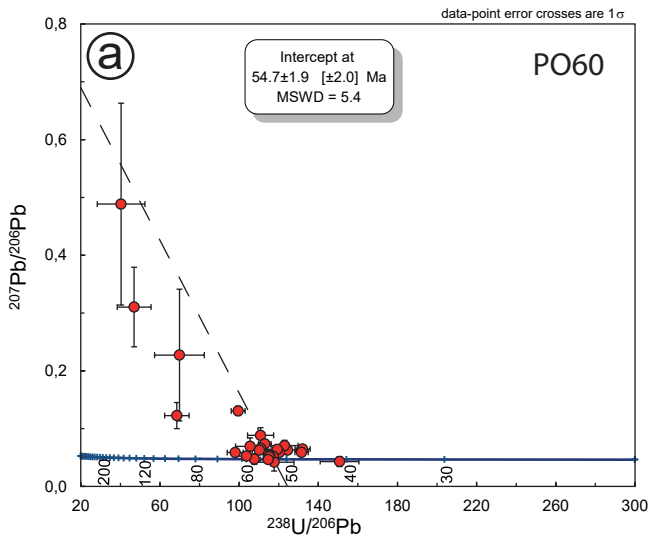


Figure 8.

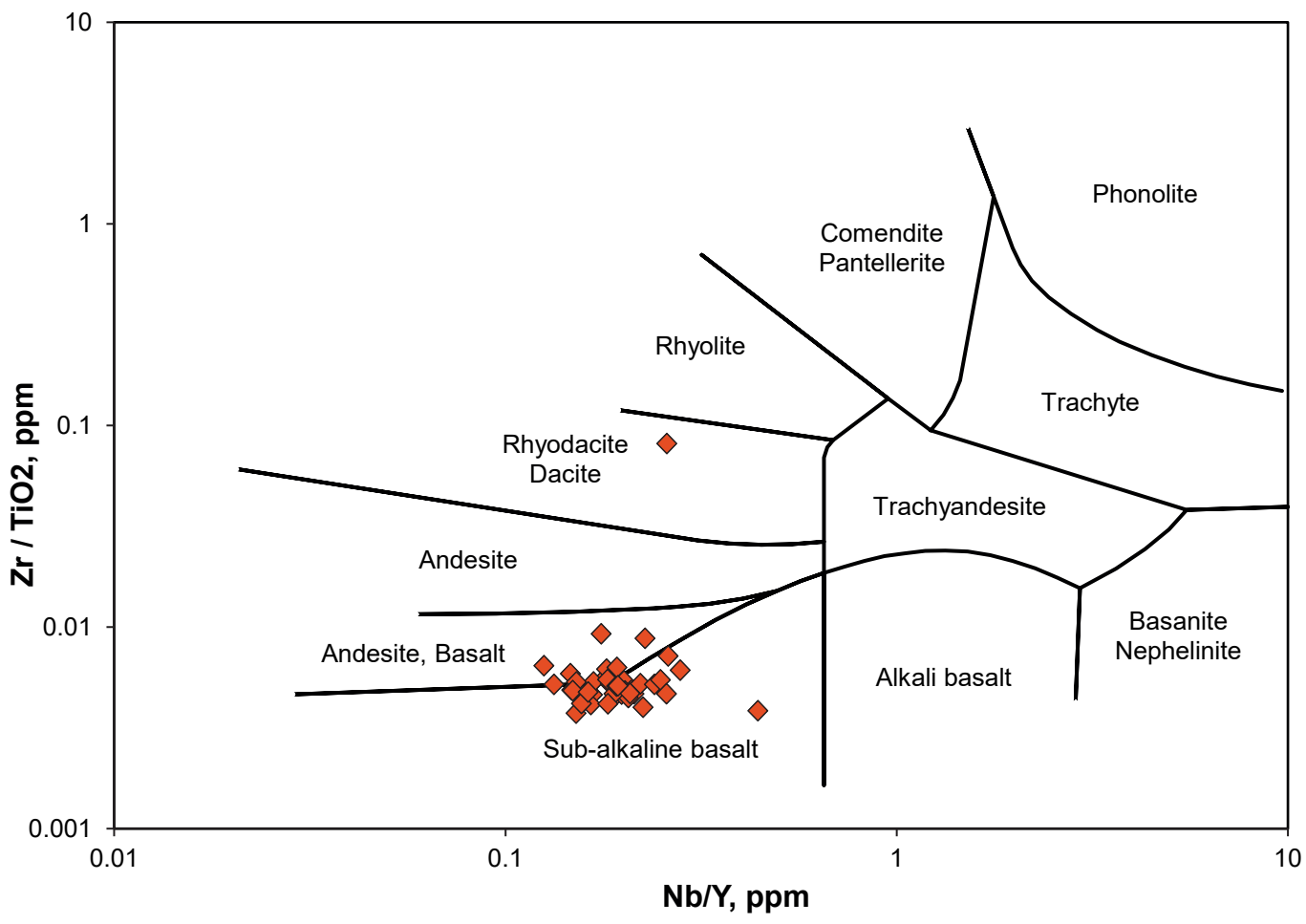


Figure 9.

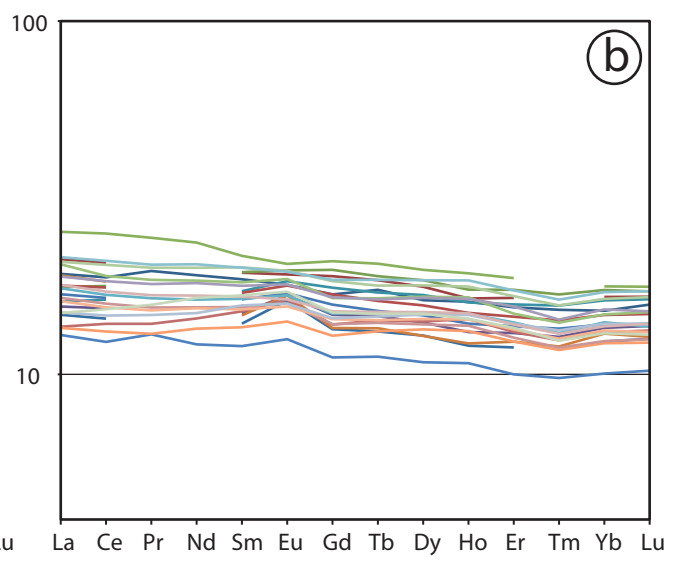
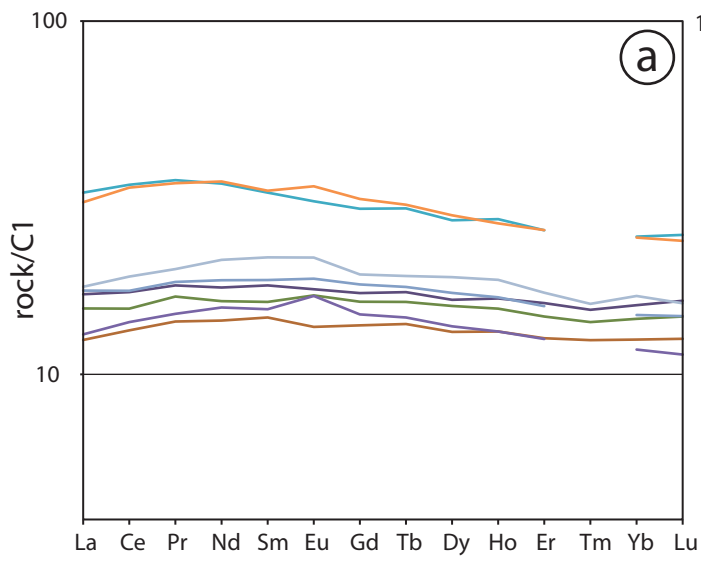


Figure 10.

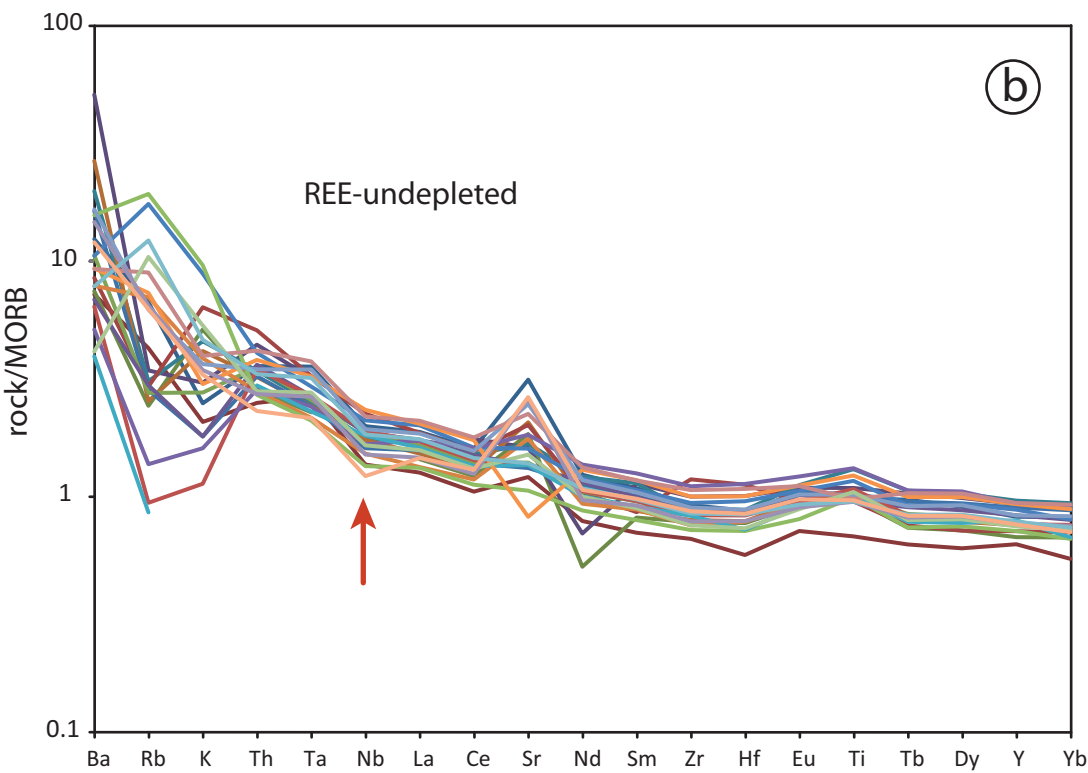
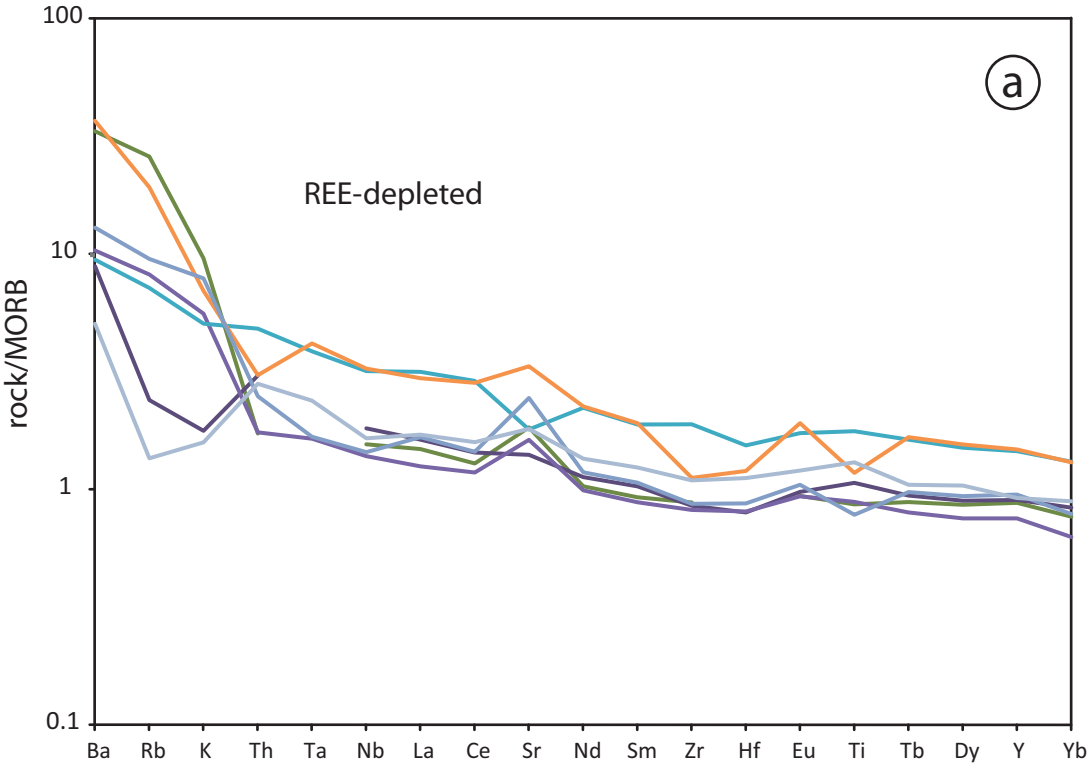


Figure 11.

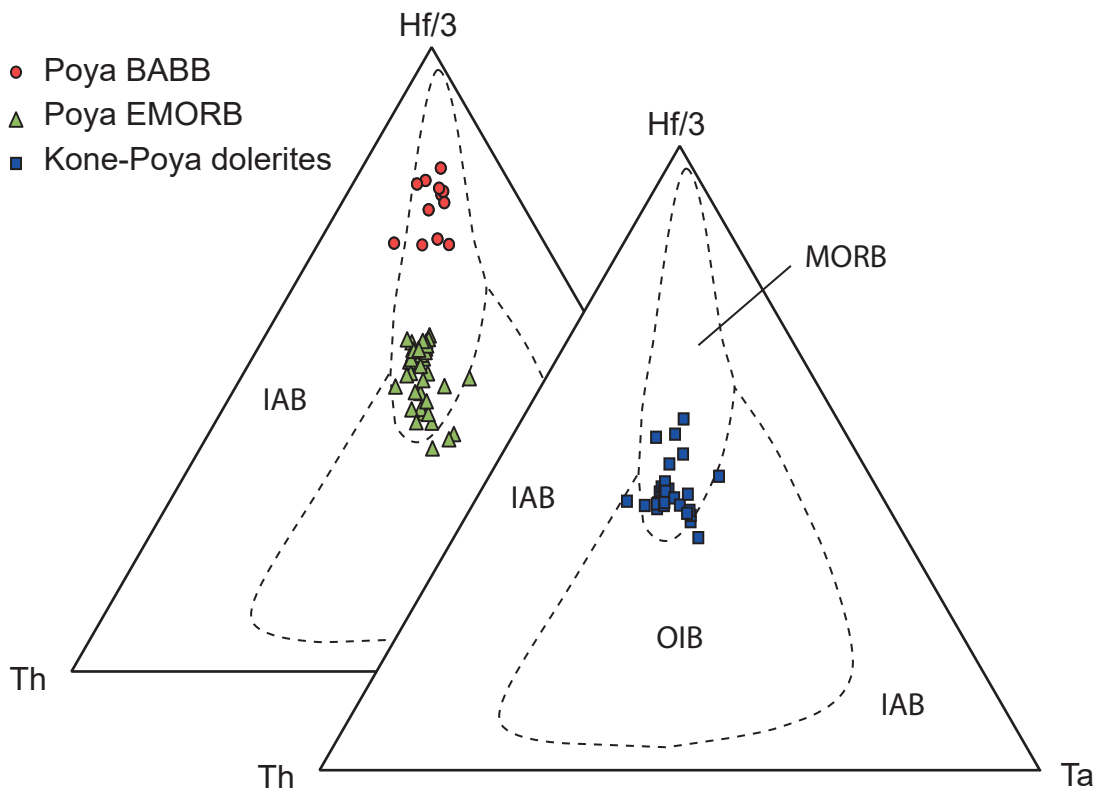


Figure 12.

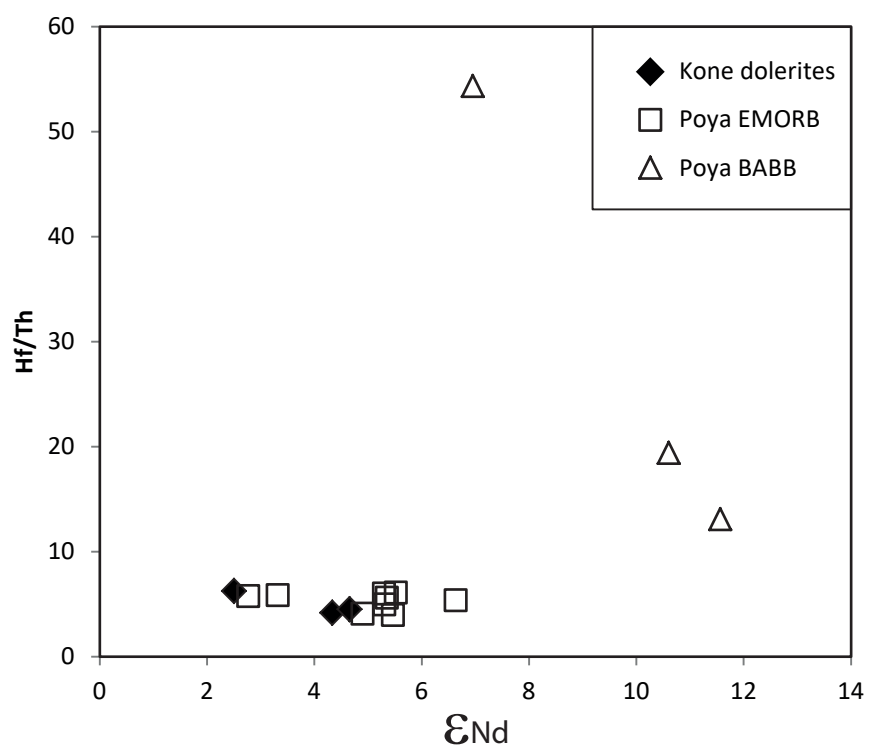
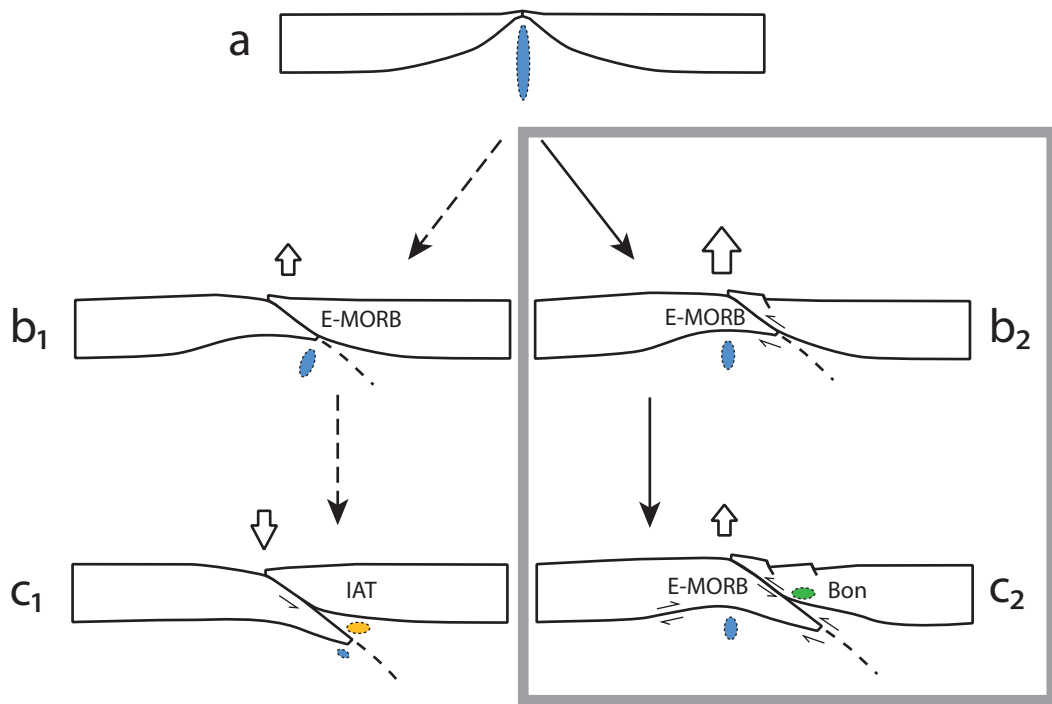


Figure 13.



-  dry melting (assuming max. depth for partial melting c.100 km)
-  hydrous melting

Figure 14.

